Emissions of trace gases and particles from savanna fires in southern Africa

Parikhit Sinha,[1] Peter V. Hobbs,[1] Robert J. Yokelson,[2] Isaac T. Bertschi,[2] Donald R. Blake,[3] Isobel J. Simpson,[3] Song Gao,[4] Thomas W. Kirchstetter,[5] and Tica Novakov[5]

Received 15 March 2002; revised 21 August 2002; accepted 22 August 2002; published 21 March 2003.

[1] Airborne measurements made on initial smoke from 10 savanna fires in southern Africa provide quantitative data on emissions of 50 gaseous and particulate species, including carbon dioxide, carbon monoxide, sulfur dioxide, nitrogen oxides, methane, ammonia, dimethyl sulfide, nonmethane organic compounds, halocarbons, gaseous organic acids, aerosol ionic components, carbonaceous aerosols, and condensation nuclei (CN). Measurements of several of the gaseous species by gas chromatography and Fourier transform infrared spectroscopy are compared. Emission ratios and emission factors are given for eight species that have not been reported previously for biomass burning of savanna in southern Africa (namely, dimethyl sulfide, methyl nitrate, five hydrocarbons, and particles with diameters from 0.1 to 3 μm). The emission factor that we measured for ammonia is lower by a factor of 4, and the emission factors for formaldehyde, hydrogen cyanide, and CN are greater by factors of about 3, 20, and 3–15, respectively, than previously reported values. The new emission factors are used to estimate annual emissions of these species from savanna fires in Africa and worldwide. *INDEX TERMS:* 0305 Atmospheric Composition and Structure: Aerosols and particles (0345, 4801); 0315 Atmospheric Composition and Structure: Biosphere/atmosphere interactions; 0322 Atmospheric Composition and Structure: Constituent sources and sinks; 0345 Atmospheric Composition and Structure: Pollution—urban and regional (0305); *KEYWORDS:* trace gas emissions, biomass fires, smoke, savanna fires, emissions from fires, particle emissions

Citation: Sinha, P., P. V. Hobbs, R. J. Yokelson, I. T. Bertschi, D. R. Blake, I. J. Simpson, S. Gao, T. W. Kirchstetter, and T. Novakov, Emissions of trace gases and particles from savanna fires in southern Africa, *J. Geophys. Res.*, *108*(D13), 8487, doi:10.1029/2002JD002325, 2003.

1. Introduction

[2] Savanna fires are the largest global source of biomass burning emissions, and tropical Africa contains about two thirds of the world's savanna [*Hao and Liu*, 1994; *Andreae et al.*, 1996]. Savanna burning is a source of a wide variety of chemical species that are important in global atmospheric chemistry, including carbon monoxide (CO), nitrogen oxides (NO_x), sulfur dioxide (SO_2), hydrocarbons, halocarbons, oxygenated organic compounds, and particles [*Delmas*, 1982; *Crutzen and Andreae*, 1990; *Ward and Hardy*, 1991; *Hurst et al.*, 1994; *Blake et al.*, 1996; *Yokelson et al.*, 1996; *Ferek et al.*, 1998]. Gases with high global warming potentials, such as methane (CH_4) and nitrous oxide (N_2O), are released in globally minor but nontrivial quantities by biomass burning [*Logan et al.*, 1981; *Quay et al.*, 1991; *Hurst et al.*, 1994; *Cofer et al.*, 1996; *Andreae et al.*, 1996]. Methyl chloride (CH_3Cl), methyl bromide (CH_3Br), and other halocarbons released by biomass burning may contribute to stratospheric ozone (O_3) depletion [*Blake et al.*, 1996; *McKenzie et al.*, 1996]. Organic and black carbon particles emitted from biomass burning play important roles in the Earth's radiation balance [*Cachier et al.*, 1996]. Gas-to-particle conversion of organic compounds, NO_x, and SO_2 may alter the radiative and cloud nucleating properties of smoke aerosols [*Reid et al.*, 1998]. Acids in smoke from biomass fires, such as acetic acid (CH_3COOH), formic acid (HCOOH), nitric acid (HNO_3), and sulfuric acid (H_2SO_4), can alter the pH of precipitation [*Lacaux et al.*, 1991; *Yokelson et al.*, 1996]. Organic compounds and CO emitted from biomass fires have been shown to react photochemically in the presence of nitrogen oxides to produce increases in ozone mixing ratios. In the case of African biomass fires, these emissions lead to widespread increases in the concentration of O_3 over the South Atlantic region [*Fishman et al.*, 1991, 1996; *Thompson et al.*, 1996].

[3] In August and September 2000, the Cloud and Aerosol Research Group (CARG) from the University of Washington (UW), with its Convair-580 research aircraft,

[1]Department of Atmospheric Sciences, University of Washington, Seattle, Washington, USA.
[2]Department of Chemistry, University of Montana, Missoula, Montana, USA.
[3]Department of Chemistry, University of California, Irvine, California, USA.
[4]Department of Chemistry, University of Washington, Seattle, Washington, USA.
[5]Lawrence Berkeley National Laboratory, Berkeley, California, USA.

0148-0227/03/2002JD002325$09.00

participated in the Southern African Regional Science Initiative 2000 (SAFARI 2000) field project. One of the goals of SAFARI 2000 is to characterize and quantify pyrogenic emissions in southern Africa. This paper focuses on this goal by using measurements obtained in numerous plume penetrations above 10 savanna fires in the tropical and subtropical regions of southern Africa (South Africa, Zambia, Mozambique, and Botswana) to derive emission ratios and emission factors for many trace gases and particles. The subsequent evolution of these trace gases and particles in the smoke from one of these fires is described by *Hobbs et al.* [2003].

2. Sampling Techniques and Instrumentation

[4] All of the measurements described in this paper were obtained aboard the UW Convair-580 research aircraft. A complete list of the instruments aboard the UW Convair-580 aircraft, and the individuals responsible for the various measurements, is given in Appendix A. Only the instruments and techniques that provided measurements presented in this paper are described here.

[5] Aerosol samples collected on quartz filters (Pallflex 2500 QAT-UP) were used to determine the concentration of particulate carbon. The quartz filters were baked before use at 800°C for at least 6 h to remove carbonaceous impurities, and then were analyzed for total carbon (TC) content using the Evolved Gas Analysis (EGA) method described by *Novakov* [1981, 1982]. In EGA, a portion of the filter is heated at a constant rate (40°C min^{-1} in this case) from 50 to 800°C in an oxygen atmosphere. The carbon-containing gases that evolve from the sample are converted to carbon dioxide (CO_2) over a manganese dioxide catalyst maintained at 800°C. The CO_2 was subsequently measured with a nondispersive infrared analyzer (Beckman Model 870). A plot of the CO_2 concentration versus temperature is called a thermogram. The area under a thermogram is proportional to the TC content of the analyzed sample. The tandem filter method described by *Turpin et al.* [1994] and *Kirchstetter et al.* [2001] was used to adjust estimates of TC for the positive sampling artifact that results from the adsorption of organic gases on the quartz filters. Black carbon (BC) concentrations were estimated with an optical transmission technique similar to that described by *Rosen and Novakov* [1983]. This method compares the attenuation of white light through a loaded filter relative to that of a blank filter. The relationship between optical attenuation (ATN) and the BC concentration ($\mu g\ cm^{-2}$) is given by $ATN = \sigma \cdot BC$, where $ATN = -100\ln(I/I_o)$, where I_o and I are the transmitted light intensities through the blank and loaded filters, respectively, and σ is the mass absorption cross-section for BC deposited on quartz ($m^2\ g^{-1}$) [*Gundel et al.*, 1984]. A value of 20 $m^2\ g^{-1}$ was used for the mass absorption cross-section. Further information on the EGA technique used here, and the results obtained, are given by *Kirchstetter et al.* [2003].

[6] Particles were also collected on Teflon (Gelman Sciences Teflo membrane, 2.0 μm pore size) filters. The Teflon filters were weighed before and after particle sampling in a humidity and temperature controlled chamber (RH = 40%, T = 293 K) to determine the masses of dry particulate matter (PM) collected on the filters. From control and field blank filters, the uncertainty of the total dry PM measured with these filters was estimated to be ±6 μg. By comparison, the typical dry PM loading for smoke aerosol samples was always greater than 100 μg.

[7] After gravimetric analysis, the particles collected on the Teflon filters were extracted in deionized water (HPLC grade) and analyzed by a standard ion chromatography system (Dionex DX 500). This analysis yielded mass concentrations of chlorine, nitrate and sulfate ions (Cl^-, NO_3^-, and SO_4^{2-}, respectively) to a precision of 5%. An Inductively Coupled Plasma-Atomic Emission Spectrometer (Jarrell Ash 955) was used to measure the mass concentration of the potassium ion (K^+) to a precision of 4%. Each of these measurements was accompanied by analysis of field blanks to correct for ambient signals. Further details on the Teflon filter analyses of aerosol compounds and the results obtained are given by *Gao et al.* [2003].

[8] The filters and SO_2 measurements often required sampling times longer than it typically took the aircraft to cross the widths of individual smoke plumes (~1–2 min). Therefore, when sampling plumes, we generally employed a "grab-bag" technique to obtain samples for the filters and SO_2. The "grab-bag" consisted of a 2.5 m^3 electrically conducting plastic (Velostat) bag that could be filled with a sample of smoke in 12 s when exposed to ram air. Samples in the grab-bag were drawn through filters for subsequent chemical analysis and mass determination of the aerosol. Various gas and aerosol instruments, such as particle size measurements normally used for real-time measurements, were configured so they could also analyze grab-bag samples. The grab-bag system had an aerosol 50% cut-off diameter of about 4 μm [*Herring*, 1994]; larger particles were lost in the inlet and on the walls of the grab bag. Nephelometric measurements indicated that aerosol mass in the grab-bag decreased by ~15% during the period of the filter sampling, presumably due to losses to the surface of the bag. Therefore, measurements of aerosol mass given here that are based on grab-bag samples may be low by up to ~15%. Grab-bag samples of ambient air were generally followed by continuous sampling of the ambient air, allowing comparisons between the two sampling techniques.

[9] Measurements of SO_2 were made on grab-bag samples using a Teco model 43S pulsed-fluorescence analyzer (precision of 7%, detection limit of 1.2 ppb). Calibration of this instrument, both in flight and on the ground, was carried out with commercial standard mixture (Scott-Marrin) of 180 ± 9 ppb SO_2 in ultra pure air. The instrument was zeroed using "pure" air (SO_2 < 1 ppb).

[10] Evacuated electropolished stainless steel canisters were used to sample smoke plumes, or ambient air just upwind of the fires, using a stainless steel inlet that passed through the aircraft fuselage. The canisters were subsequently analyzed for hydrocarbons, halocarbons, dimethyl sulfide (DMS), and methyl nitrate (CH_3ONO_2). The mixing ratios of species obtained in the ambient air were subtracted from the corresponding mixing ratios measured in the smoke samples to obtain excess mixing ratios. The canisters filled in ~30 s at a nonlinear rate.

[11] For each whole air sample, mixing ratios of selected C_2-C_{11} nonmethane hydrocarbons (NMHC), methyl chloride (CH_3Cl), methyl iodide (CH_3I), and methyl bromide (CH_3Br) were determined by gas chromatography (GC) with flame ionization detection (FID) and electron capture

detection (ECD). The precision of the NMHC and methyl halide measurements was 3%, and the typical NMHC detection limit 3 pptv. Mixing ratios of CO_2 (precision of 3%), CO (precision of 5%), and CH_4 (precision of 0.1%) in the canisters were determined using a second GC/FID. A detailed description of the analytical procedure for the whole air samples, including quantification of the measurement precision for individual compounds, is given by *Colman et al.* [2001].

[12] An Airborne Fourier Transform Infrared spectrometer (AFTIR) was deployed onboard with a separate and specially coated inlet that directed ram air through a Pyrex multipass cell with an exchange time of 4–5 s. AFTIR acquired the infrared spectrum of the cell contents every 0.83 s allowing water vapor (H_2O), CO_2, CO, and CH_4 to be measured continuously. For the plume penetrations, the AFTIR was used to detain smoke samples for 2–3 min of signal averaging, which allowed measurements of most reactive and stable trace gases that were present above 5–20 ppbv. The gases were H_2O, CO_2, CO, nitric oxide (NO), nitrogen dioxide (NO_2), CH_4, ethene (C_2H_4), acetylene (C_2H_2), formaldehyde (HCHO), methanol (CH_3OH), acetic acid (CH_3COOH), formic acid (HCOOH), ammonia (NH_3), O_3, and hydrogen cyanide (HCN). This provided a rare capability to measure several important gases by two independent methods. The AFTIR technique and results are described in detail by *Yokelson et al.* [2003].

[13] The total concentrations of particles in the size range 0.003–3 μm diameter were measured with a TSI 3025A ultrafine condensation particle counter (precision of 10%). A Particle Measuring Systems (PMS) passive cavity aerosol spectrometer probe (PCASP-100X) was also used for measuring particle size spectra. The PCASP-100X is an optical particle counter that was mounted on the wing of the aircraft. The sampling inlet was heated to dry the particles, so that measurements from the PCASP could be compared with those obtained on dried particles with other instruments inside the aircraft cabin. The PCASP-100X was regularly calibrated on the ground using polystyrene latex spheres of known sizes. A differential mobility particle sizer (DMPS) was used to measure aerosol size spectra from 0.01–0.6 μm diameter [*Winklmayer et al.*, 1991]. Since this instrument requires a 2–4 min analysis time, it was fed from the grab bag.

3. Definition and Calculation of Excess Molar Mixing Ratio, Normalized Excess Molar Emission Ratio, Emission Factor, and Combustion Efficiencies

[14] The excess molar or volume mixing ratio, ΔX, of a species X in a smoke plume is defined as:

$$\Delta X = X_{plume} - X_{ambient} \quad (1)$$

where, X_{plume} and $X_{ambient}$ are the molar or volume mixing ratios of X in the smoke plume and in the ambient air, respectively.

[15] The normalized excess molar emission ratio of a species X, ER(X), is the excess molar or volume mixing ratio of X divided by the excess molar or volume mixing ratio of a reference tracer (such as CO or CO_2) measured close to a fire. For example, the normalized excess molar emission ratio of species X relative to CO is:

$$ER(X) = \frac{\Delta X}{\Delta CO} \quad (2)$$

The normalized excess molar emission ratio can be obtained from the slope of the regression line between the excess mixing ratio of X (e.g., excess values of X in ppmv) and the excess mixing ratio of the reference tracer.

[16] Emission factors for gases and particles were calculated using the carbon mass balance method [*Radke et al.*, 1988; *Ward and Radke*, 1993]. The underlying premise of this method is that all of the carbon combusted in a fire and released to the atmosphere is emitted into the smoke plume as CO_2, CO, CH_4, nonmethane organic carbon (NMOC), and particulate carbon (PC). The emission factor (EF) of a species X is defined here as the ratio of the excess mass concentration [ΔX] of X emitted by a fire to the excess mass concentration of total carbon, [ΔC], emitted by the fire:

$$EF(X) = \frac{[\Delta X]}{[\Delta C]_{CO_2} + [\Delta C]_{CO} + [\Delta C]_{CH_4} + [\Delta C]_{NMOC} + [\Delta C]_{PC}} \quad (3)$$

The emission factor is expressed in units of grams of X emitted per kilogram of carbon burned. To convert this emission factor to units of grams of X emitted per kilogram of fuel burned, EF is multiplied by the mass fraction of carbon in the fuel. Typically, the carbon content of biomass fuels varies from 45 to 55% [*Susott et al.*, 1996]. In this study, we assume that it is 50%.

[17] The combustion efficiency (CE) is the molar ratio of excess carbon (C) emitted as CO_2 from a fire to the total excess carbon emitted [*Ward and Hardy*, 1991]:

$$CE = \frac{\Delta C_{CO_2}}{\Delta C_{CO_2} + \Delta C_{CO} + \Delta C_{CH_4} + \Delta C_{NMOC} + \Delta C_{PC}} \quad (4)$$

Thus, CE is the molar fraction of fuel carbon emitted that is completely oxidized to CO_2.

[18] Although CE is a useful quantity for fire models, it is often difficult to measure all of the individual carbon species in the emissions from a fire. Therefore, in this study we have chosen to use the modified combustion efficiency (MCE) as the principal quantity to describe the relative amounts of flaming and smoldering combustion [*Ward and Hao*, 1992; *Ward and Radke*, 1993], which is defined as:

$$MCE = \frac{\Delta C_{CO_2}}{\Delta C_{CO_2} + \Delta C_{CO}} \quad (5)$$

Since CH_4, NMOC and PC are emitted in relatively small quantities compared to CO_2 and CO, the difference between CE and MCE is typically only a few percent.

[19] Both CE and MCE are useful as indicators of the relative amounts of flaming and smoldering combustion that generate emissions. In laboratory studies, *Yokelson et al.* [1996] found that pure flaming combustion has an MCE near 0.99 and pure smoldering combustion an MCE of ~0.8. Therefore, an MCE <0.9 suggests >50% smoldering combustion, and an MCE >0.9 suggests >50% flaming

combustion. In this study, the average MCE measured independently by the AFTIR (0.94) and the canister sampling (0.94) both show that the savanna fires sampled were often dominated by flaming combustion.

4. Vegetative Types and Sampling of Smoke

[20] The nature of the vegetative fuel plays an important role in determining emissions from biomass fires [e.g., *Ward and Hardy*, 1991]. We report here on measurements obtained in the smoke from 10 fires covering a variety of vegetation types in several regions of southern Africa (Table 1): four fires in South Africa, two in Zambia, one in Mozambique, and three on the Botswana/South Africa border. Vegetation types varied from lowvelds and highvelds in South Africa, to dambo and miombo woodlands in Zambia, to east African coastal mosaic in Mozambique. The lowveld fires were located in and around the Kruger National Park in South Africa. Vegetation in the lowvelds varied from south Zambezian undifferentiated woodland to Tongaland-Pondoland bushland [*White*, 1981, 1983]. The bushveld fires were located on the Botswana/South Africa border, in a Zambezian vegetation zone that transitions from undifferentiated woodland to Acacia deciduous bushland and wooded grassland. The miombo woodland fires in Zambia were in a Zambezian woodland vegetation zone dominated by species of Brachystegia and related genera. The dambo grassland fire in Zambia was in a seasonally flooded region covered with a medium-dense, uniform grass mat. The Mozambique fire was located in a transition zone between miombo woodland dominated by Brachystegia and a Zanzibar-Inhambane east African coastal mosaic of woodland habitats [*White*, 1981, 1983].

[21] More than 60 penetrations were made through the smoke plumes of the 10 fires. However, to determine emission factors, we use only the results for smoke samples less than a few minutes old acquired directly (typically ~500 m) above the fires, which we term "initial" smoke. Canisters were filled and grab-bag samples acquired during 16 penetrations of initial smoke.

5. Results and Discussion

[22] In this section we present emission ratios and emission factors for biomass burning in southern Africa of 50 gaseous and particulate species, including CO_2, CO, NO_x, SO_2, oxygenates, hydrocarbons, halocarbons, ionic aerosols, and carbonaceous aerosols. These emissions affect the atmosphere in several important ways: greenhouse warming, the oxidizing capacity and acidity of the troposphere, stratospheric ozone depletion, and light scattering and absorption. Although much of the CO_2 released in savanna fires is sequestered as vegetation grows back, this is not the case for the greenhouse gas CH_4. Furthermore, CO released from fires is oxidized to CO_2 through reacting with OH, thus depleting the main sink for CH_4 and lengthening its lifetime. Thus, CO released from biomass burning has indirect effects on global warming. Emissions of nitrogen oxides, organic compounds, and CO from biomass burning result in the formation of O_3, another important greenhouse gas.

Table 1. Savanna Fires in Southern Africa From Which Measurements Were Obtained in This Study

Name of Fire and/or General Location	Latitude, °S	Longitude, °E	Date, mm:dd:yy	Time, UTC	Number of Samples (GC/C, AFTIR)	Country	Vegetation Type	Type of Fire	Modified Combustion Efficiency (MCE),[a] %
Skukuza 1 (Kruger National Park, South Africa)	25.46	31.58	08:17:00	1002	1, 3	South Africa	Lowveld	Fire of opportunity	93.8
Skukuza 2 (Kruger National Park, South Africa)	24.43	31.83	08:17:00	1110	1, 3	South Africa	Lowveld	Fire of opportunity	97.9
Madikwe 1 (Game Reserve in the Limpopo River valley, South Africa)	24.67	26.41	08:18:00	916	1, 5	South Africa, Botswana border	Bushveld	Prescribed fire	89.7
Madikwe 2 (Game Reserve in the Limpopo River valley, South Africa)	24.74	26.24	08:20:00	1253	1, 2	South Africa, Botswana border	Bushveld	Prescribed fire	98.0
Madikwe 3 (Game Reserve in the Limpopo River valley, South Africa)	24.66	26.29	08:20:00	1328, 1354	2, 3	South Africa, Botswana border	Bushveld	Prescribed fire	93.7, 92.1
Kruger National Park (South Africa)	25.10	31.46	08:29:00	1410, 1417	2, 2	South Africa	Lowveld	Fire of opportunity	92.7, 90.0
Beira (Mozambique)	21.00	34.74	08:31:00	1119, 1133	2, 3	Mozambique	Miombo woodland/ East African Coastal Mosaic	Fire of opportunity	94.8, 92.4
Kaoma 1 (Zambia)	14.81	24.48	09:01:00	0902, 0908	2, 6	Zambia	Miombo woodland	Prescribed fire	93.6, 93.8
Kaoma 2 (Zambia)	14.84	24.43	09:05:00	1156, 1208	2, 5	Zambia	Dambo grassland	Prescribed fire	96.1, 96.7
Timbavati (Near Kruger National Park, South Africa)	24.37	31.22	09:07:00	0842, 0857	2, 4	South Africa	Lowveld	Prescribed fire	93.8, 92.9

[a]Derived from the canister/gas chromatograph measurements.

[23] We report here emission ratios and emission factors for precursors of the primary oxidants in the atmosphere, namely, OH and O_3. Photolysis of O_3 in the presence of water vapor will lead to the formation of OH. Photolysis of formaldehyde released from biomass fires will produce OH and lead to O_3. The oxidants produced in aged smoke will eventually be depleted by reactions with the CO and CH_4 released in the fires. Also given here are emission ratios and emission factors for halocarbons, which can eventually serve as sources for chlorine or bromine in the stratosphere where they will catalyze stratospheric O_3 depletion.

[24] Emission ratios and emission factors are given for aerosols that scatter and/or absorb solar radiation. Inorganic and organic aerosols scatter solar radiation, reducing the downwelling flux available for photochemistry and warming of the Earth's surface. Black carbon absorbs solar radiation, which warms layers of the atmosphere, creating vertical stability below them that can confine pollutants near the surface. Ions, such as sulfate and nitrate, either released from fires or formed through the oxidation of SO_2 and NO_x, can be removed from the atmosphere by either dry or wet deposition, thereby acidifying precipitation and soils. Acetic and formic acid, released from fires or formed through the oxidation of hydrocarbons, will also affect the pH of precipitation and soils. Emission of positive ions, such as K^+, and the formation of NH_4^+ from NH_3 released from biomass fires, can partly neutralize these acids.

[25] It should be emphasized that the emission ratios and emission factors given here are based on measurements made in smoke just above the fires (i.e., initial smoke). Many of the emissions undergo transformations as the smoke ages, as discussed by *Hobbs et al.* [2003].

[26] It is beyond the scope of this paper to discuss all aspects of the large data set reported here. Instead we will focus on those species that have not been previously estimated or measured, and those species for which the emission ratios and emission factors derived from our measurements differ significantly from those reported in earlier studies. (We define "significant" as a statistical confidence level $\geq$95%.) It should also be noted that many more species were measured than are reported here. In this paper, a species was considered to be emitted from a fire only if the correlation coefficient (r^2) for the excess mixing ratio of that species against the excess mixing ratio of CO (or CO_2) was $\geq$0.5.

5.1. Emission Ratios

[27] The excess molar mixing ratio of each species was regressed against the excess molar mixing ratio of CO or CO_2 to obtain the emission ratio of that species. The slope of the regression line gives the molar emission ratio (hereafter abbreviated to "emission ratio") of the species with respect to the reference tracer (CO or CO_2). Since NO_x, SO_2, and CO_2 are mainly emitted in flaming combustion, excess values of NO_x and SO_2 were regressed against excess CO_2. Other compounds are mainly emitted with CO during smoldering combustion, so their excess mixing ratios were regressed against excess CO.

[28] Figure 1 shows the excess mixing ratios of several species plotted against excess mixing ratios of CO (or CO_2). Slopes and correlation coefficients for these and all the other species we measured are listed in Table 2 (for the canister samples) and in Table 3 (for the AFTIR samples). For emission ratios obtained from the gas chromatography measurements (Table 2), an average emission ratio for a given species was derived using the sixteen canister samples from the 10 fires. For the AFTIR measurements (Table 3), there were often several measurements close to the fire in each of the smoke plumes. For these cases, we give an average emission ratio for each measured species for each fire. The average emission ratios of CO, CH_4, and acetylene in Table 2 are not significantly different from the corresponding values listed in Table 3. However, the average emission ratio for ethene determined from the AFTIR is about 50% greater than that determined from gas chromatography. In section 6 of this paper we compare and discuss measurements obtained by gas chromatography with those obtained by AFTIR. Emission ratios are not given here for O_3 since, although O_3 develops downwind in smoke plumes, it is not emitted directly from a fire. The time evolution of O_3 in one of the smoke plumes we studied is described by *Hobbs et al.* [2003].

[29] For comparison with our measurements, we also show in Table 2 the emission ratios for smoke from savanna fires in southern Africa and agricultural fires in Brazil reported by *Blake et al.* [1996], and for smoke from grass, cerrado and forest fires in Brazil given by *Ferek et al.* [1998]. The analysis techniques used in these two studies were similar to those we used in Africa. The sampling by *Blake et al.* [1996] in Africa was conducted in September–October 1992, similar to the August–September period of SAFARI 2000. However, most of the samples collected by Blake et al. were of aged smoke, whereas, the measurements reported here and those of Ferek et al. are for initial smoke.

[30] Blake et al. reported emission ratios for CH_4 with respect to CO of 0.078 ± 0.004 and 0.094 ± 0.013 for southern Africa and Brazil, respectively. For Brazil, Ferek et al. report a CH_4 emission ratio of 0.12. Our emission ratios for CH_4 in southern Africa are 0.039 ± 0.003 for samples collected in canisters and 0.053 ± 0.012 from the AFTIR measurements. It appears from the average of these measurements that the CH_4 emission ratio with respect to CO from biomass burning in Brazil (0.11 ± 0.02) may be greater than that for savanna burning in southern Africa (0.057 ± 0.013). This could be due to high CH_4 emissions for downed woody material [*Bertschi et al.*, 2003].

[31] We found a stronger correlation between excess CH_3Br and excess CO (r^2 = 0.69) than between excess CH_3I and excess CO (r^2 = 0.50) (Table 2). The emission ratios for CH_3Br, CH_3Cl and CH_3I reported here are 10–40% lower than those reported by *Blake et al.* [1996] for African biomass fires, and 30–66% lower than those reported by Blake et al. for Brazilian fires. *Mano and Andreae* [1994] estimated that CH_3Br emissions from biomass burning worldwide range from 10 to 50 Gg per year, which is comparable to that from oceans and pesticide use. Their value was obtained using a methyl bromide-to-methyl chloride emission ratio of 6×10^{-3} to 9×10^{-3}. Based on the measurements reported here for savanna burning in southern Africa, the emission ratio of methyl bromide with respect to methyl chloride is $(7.5 \pm 0.6) \times 10^{-3}$ (Figure 2), which lies within the range used by Mano and Andreae.

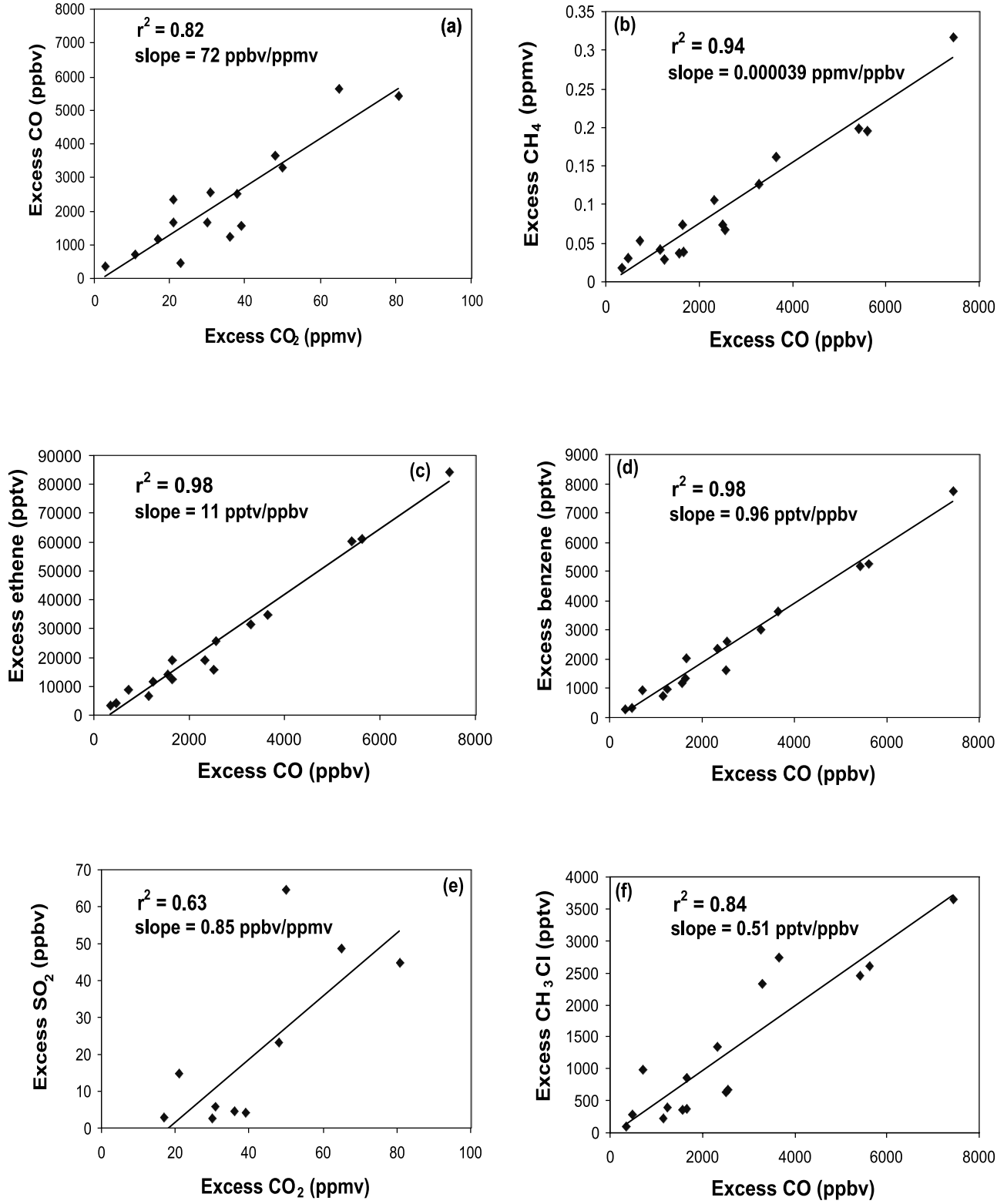

Figure 1. Excess mixing ratios of selected trace gases (measured in canisters) versus excess mixing ratios of CO_2 or CO in the smoke from savanna fires in southern Africa. The correlation coefficient is given by r^2.

[32] S. Meinardi et al. (Dimethyl disulfide and dimethyl sulfide emissions from biomass burning, submitted to *Geophysical Research Letters*, 2002) detected emissions of dimethyl sulfide (CH_3SCH_3 or DMS) from bush fires in Australia. Their molar emission ratio of DMS to CO was 6.3×10^{-6}. The mixing ratios of DMS in southern Africa smoke plumes are strongly correlated with CO (Table 2 and Figure 3). This confirms that biomass burning is a source of

Table 2. Average Molar Emission Ratios (With Respect to CO or CO_2) Measured in This Study for Initial Smoke From Savanna Fires in Southern Africa for Which the Correlation Coefficients (r^2) of the Excess Mixing Ratios of the Species Versus the Excess Mixing Ratio of CO or CO_2 was Greater Than or Equal to 0.5, and Which Were Therefore Considered to be Emitted by the Fires[a]

Species	Technique Used for Measurement in This Study[b]	Southern Africa (This Study)		Southern Africa [*Blake et al.*, 1996]		Brazil [*Blake et al.*, 1996]		Brazil [*Ferek et al.*, 1998]	
		Molar Emission Ratio	r^2	Molar Emission Ratio	r^2	Molar Emission Ratio	r^2	Molar Emission Ratio	r^2
Carbon monoxide (CO)	GC/C	0.072 ± 0.009	0.82	–	–	–	–	–	–
Methane (CH_4)	GC/C	0.039 ± 0.003	0.94	0.078 ± 0.004	0.91	0.094 ± 0.013	0.70	0.12	0.90
Sulfur dioxide (SO_2)	Teco 43S (via bag house)	0.00085 ± 0.0002	0.63	–		–		–	
Dimethyl sulfide (CH_3SCH_3)	GC/C	0.0000087 ± 0.0000011	0.86	–		–		–	
Methyl bromide (CH_3Br)	GC/C	0.0000036 ± 0.0000006	0.69	0.0000060 ± 0.0000005	0.78	0.0000106 ± 0.0000008	0.88	–	–
Methyl chloride (CH_3Cl)	GC/C	0.00051 ± 0.00006	0.84	0.00057 ± 0.00003	0.92	0.00085 ± 0.00006	0.88	–	–
Methyl iodide (CH_3I)	GC/C	0.00000084 ± 0.00000023	0.50	0.0000012 ± 0.0000002	0.70	0.0000012 ± 0.0000002	0.57	–	–
Methyl nitrate (CH_3ONO_2)	GC/C	0.0000025 ± 0.0000004	0.74	–	–	–	–	–	–
Ethane (C_2H_6)	GC/C	0.0026 ± 0.00022	0.93	0.0052 ± 0.0002	0.96	0.0083 ± 0.0003	0.97	0.0052	0.85
Ethene (C_2H_4)	GC/C	0.0110 ± 0.0005	0.98	0.0083 ± 0.0006	0.78	0.0061 ± 0.0004	0.87	0.011	0.83
Propane (C_3H_8)	GC/C	0.00048 ± 0.00006	0.81	0.00097 ± 0.00004	0.94	0.0016 ± 0.001	0.95	0.0010	0.82
Propene (C_3H_6)	GC/C	0.0028 ± 0.0002	0.94	0.001 ± 0.0001	0.56	0.0004 ± 0.0001	0.62	0.0039	0.87
Acetylene (C_2H_2)	GC/C	0.0032 ± 0.0003	0.92	0.0045 ± 0.0001	0.98	0.0033 ± 0.0001	0.97	0.0024	0.63
i-butane (C_4H_{10})	GC/C	0.000031 ± 0.000004	0.82	0.000043 ± 0.000004	0.77	0.000055 ± 0.000010	0.55	–	–
n-butane (C_4H_{10})	GC/C	0.000087 ± 0.0000074	0.92	0.00016 ± 0.00001	0.88	0.00021 ± 0.00002	0.86	0.00021	0.79
t-2-butene (C_4H_8)	GC/C	0.00012 ± 0.0000098	0.92	–	–	–	–	0.00026	0.89
1-butene (C_4H_8)	GC/C	0.00042 ± 0.000036	0.91	–	–	–	–	0.00066	0.90
c-2-butene (C_4H_8)	GC/C	0.000086 ± 0.0000071	0.92	–	–	–	–	0.00022	0.89
n-pentane (C_5H_{12})	GC/C	0.000017 ± 0.0000046	0.51	0.000053 ± 0.000005	0.80	0.000051 ± 0.000005	0.80	0.000059	0.73
1, 3-butadiene (C_4H_6)	GC/C	0.00048 ± 0.000044	0.90	–	–	–	–	–	–
3-methyl-l-butene (C_5H_{10})	GC/C	0.000033 ± 0.000003	0.94	–	–	–	–	–	–
t-2-pentene (C_5H_{10})	GC/C	0.000032 ± 0.0000027	0.92	–	–	–	–	–	–
2-methyl-2-butene (C_5H_{10})	GC/C	0.000026 ± 0.0000025	0.90	–	–	–	–	–	–
2-methyl-1-butene (C_5H_{10})	GC/C	0.000033 ± 0.0000022	0.95	–	–	–	–	–	–
c-2-pentene (C_5H_{10})	GC/C	0.000021 ± 0.0000014	0.95	–	–	–	–	–	–
n-hexane (C_6H_{14})	GC/C	0.000055 ± 0.0000042	0.94	–	–	–	–	–	–
Isoprene (C_5H_8)	GC/C	0.00017 ± 0.000043	0.53	–	–	–	–	0.000069	0.73
2-methyl-1-pentene (C_6H_{12})	GC/C	0.000026 ± 0.0000022	0.92	–	–	–	–	–	–
n-heptane (C_7H_{16})	GC/C	0.000025 ± 0.0000024	0.90	–	–	–	–	–	–
Benzene (C_6H_6)	GC/C	0.00096 ± 0.00004	0.98	0.00130 ± 0.00004	0.96	0.00129 ± 0.00005	0.97	0.0015	0.89
Toluene(C_7H_8)	GC/C	0.00072 ± 0.000074	0.87	0.00049 ± +0.00003	0.85	0.00057 ± 0.00003	0.93	0.00094	0.81
Sum of all NMHC listed above	GC/C	0.024 ± 0.001	0.98	0.022	–	0.022	–	0.027	–
Total particulate matter (TPM)[c]	F/GB	200 ± 66	0.69	–	–	–	–	–	–
Organic carbon (OC)	F/GB	32 ± 12	0.56	–	–	–	–	–	–
Black carbon (BC)	F/GB	6 ± 2.2	0.55	–	–	–	–	–	–
Total carbon (TC)	F/GB	40 ± 12	0.60	–	–	–	–	–	–
Chloride (Cl^-)	F/GB	32 ± 14	0.58	–	–	–	–	–	–
Nitrate (NO_3^-)	F/GB	3.3 ± 0.63	0.88	–	–	–	–	–	–
Sulfate (SO_4^{2-})	F/GB	4.4 ± 1.6	0.66	–	–	–	–	–	–
Potassium (K^+)	F/GB	15 ± 3.8	0.79	–	–	–	–	–	–

[a]Shown for comparison are results from *Blake et al.* [1996] for mainly aged smoke from savanna fires in southern Africa and from agricultural fires in Brazil, and from *Ferek et al.* [1998] for young smoke from grass, cerrado, and forest fires in Brazil. Molar emission ratios were obtained from the slope of the excess mixing ratio of a species plotted against the excess mixing ratio of a reference species. For CO and SO_2, the reference species was CO_2; for all other compounds, the reference species was CO. Molar emission ratios have no units, except for particles (i.e., TPM and thereafter) for which the units are excess $\mu g/m^3$/excess CO ppmv.

[b]GC/C = gas chromatography via canisters; F/GB = filters via grab bag.

[c]For particles up to ~4 μm diameter.

Table 3. As for Table 2 But for Smoke From Some of the Individual Savanna Fires Sampled by AFTIR in Southern Africa in This Study[a]

Species	Skukuza 1, 2	Madikwe 1	Madikwe 2, 3	Kruger National Park	Beira	Kaoma 1	Kaoma 2	Timbavati	Average ± Standard Deviation From This Study
Carbon monoxide (CO)/CO_2	0.078	0.059	0.046	0.073	0.099	0.063	0.026	0.069	0.064 ± 0.022
Nitric oxide (NO)/CO_2	0.0019	0.0019	0.001	0.0011	–	0.0010	0.0009	0.0008	0.0011 ± 0.0004
Nitrogen dioxide (NO_2)/CO_2	0.0016	0.0020	0.0022	0.0019	0.0030	0.0020	0.0011	0.0018	0.0020 ± 0.0005
Methane (CH_4)/CO	0.059	0.054	0.048	0.070	0.061	0.036	0.038	0.059	0.053 ± 0.012
Ethene (C_2H_4)/CO	0.019	0.015	0.020	0.016	0.016	0.012	0.023	0.016	0.017 ± 0.003
Acetylene (C_2H_2)/CO	0.0033	0.0037	0.0054	0.0043	0.0037	0.0037	0.0072	0.0034	0.0043 ± 0.0013
Formaldehyde (HCHO)/CO	0.016	0.014	0.023	0.010	0.013	0.010	0.012	0.019	0.015 ± 0.004
Methanol (CH_3OH)/CO	0.014	0.016	0.015	0.020	0.014	0.013	0.0093	0.015	0.015 ± 0.003
Acetic acid (CH_3CO_2H)/CO	0.019	0.017	0.017	0.017	0.016	0.015	0.013	0.015	0.016 ± 0.002
Formic acid (HCO_2H)/CO	0.0021	0.0066	0.0087	0.0054	0.0045	0.0051	0.0087	0.0064	0.0059 ± 0.0022
Ammonia (NH_3)/CO	0.0076	0.0081	0.012	0.0027	–	0.0097	–	0.0016	0.0070 ± 0.0046
Hydrogen cyanide (HCN)/CO	0.0094	0.011	0.013	0.0059	0.0056	0.056	0.011	0.0072	0.0085 ± 0.0029

[a]See Table 1 for information on each fire.

DMS. Using our value for the molar emission ratio of DMS with respect to CO [$(8.7 \pm 1.1) \times 10^{-6}$], together with an estimate for the annual emission of CO worldwide from savanna and grassland burning (206 Tg yr^{-1} [*Andreae and Merlet*, 2001]), yields an annual flux of DMS from savanna and grassland burning of 2.9 ± 0.4 Gg yr^{-1}. For comparison, the annual flux of DMS from the world's oceans is 30–50 Tg yr^{-1} [*Seinfeld and Pandis*, 1998]. However, there are large uncertainties associated with this type of extrapolation, in which a small number of data points from a specific region and season are used as a surrogate for DMS emissions from global savanna and grassland burning throughout the year. Also, there are significant uncertainties in the global CO emission estimates, which are known to within only about ±50% [*Blake et al.*, 1996].

[33] Although small in relation to marine sources, DMS from biomass burning could be an important source of sulfur in nonindustrial, continental interiors, even though direct emissions of sulfur as SO_2 from biomass burning (0.43 ± 0.30 g kg^{-1} for savanna burning in southern Africa) dominates over that of DMS (0.0013 ± 0.0011 g kg^{-1}). Oxidation of DMS by OH leads to the formation of SO_2. The lifetime of DMS with respect to OH oxidation is ~2 days [*Warneck*, 2000]. On the other hand, the lifetime of SO_2 with respect to removal by dry deposition is only ~1 day [*Seinfeld and Pandis*, 1998]. Therefore, DMS will be transported over larger distances after which, following oxidation by OH, it will serve as a source of SO_2.

[34] The AFTIR aboard the Convair-580 in SAFARI 2000 provided the first quantitative measurements of oxygenated organic compounds in smoke from savanna fires (Table 3). The emission ratios of these compounds show that 3 of the top 5 organic compounds emitted by savanna fires are oxygenated. These compounds are discussed further in section 5.2 of this paper and by *Yokelson et al.* [2003].

[35] Many other species measured in this study show potentially interesting results, but are not included in our tabulations or discussion because they did not satisfy our criteria for being emitted from the biomass fires (i.e., a

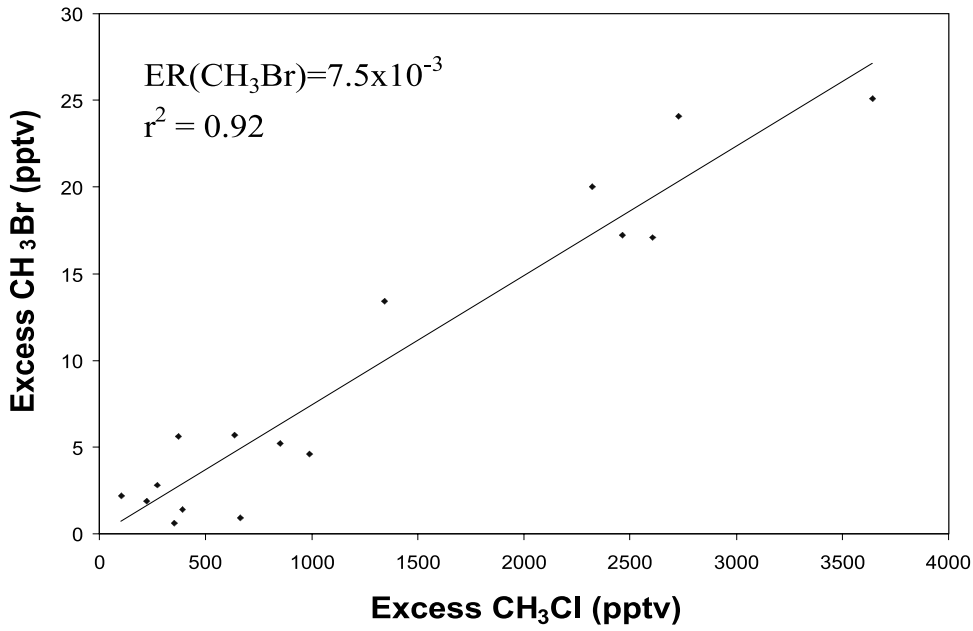

Figure 2. Excess mixing ratio of methyl bromide versus excess mixing ratio of methyl chloride. The molar emission ratio (ER) for methyl bromide with respect to methyl chloride obtained from the slope of the plot is shown. The correlation coefficient is given by r^2.

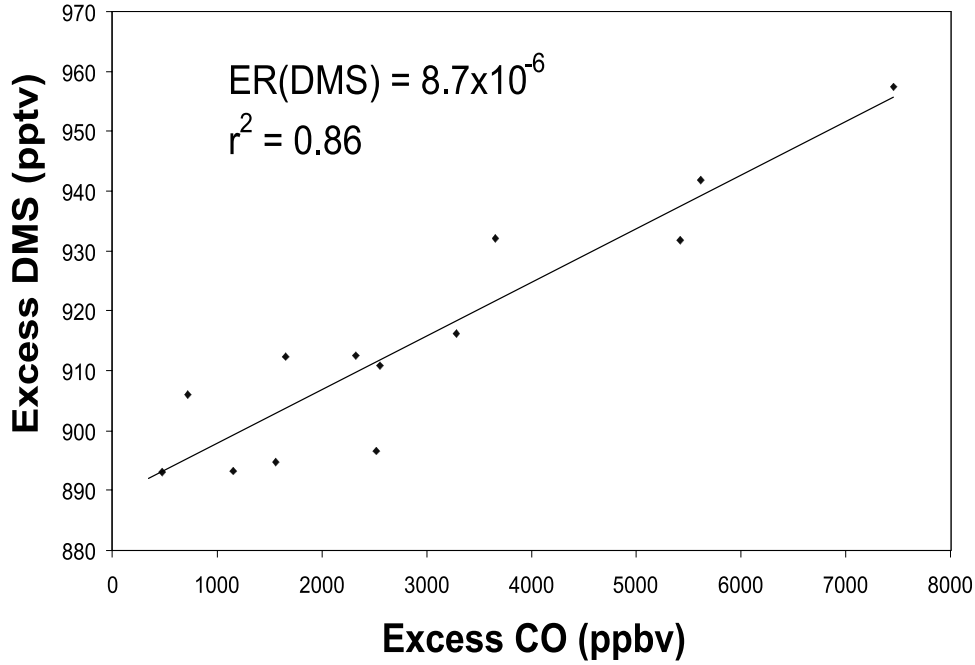

Figure 3. Excess mixing ratios of DMS versus excess mixing ratios of CO. The molar emission ratio (ER) for DMS with respect to CO obtained from the slope of the plot is shown. The correlation coefficient is given by r^2.

correlation coefficient $\geq$0.5 for the excess mixing ratio of the species against the excess mixing ratio of CO or CO_2). For example, based on our measurements, the emission ratio of *i*-pentane with respect to excess CO in the smoke was about a factor of 5 below that reported by *Ferek et al.* [1998]. However, the correlation coefficient for the excess mixing ratio of *i*-pentane against the excess mixing ratio of CO was 0.43.

5.2. Emission Factors

[36] All of the emission factors (EF) reported here are based on airborne measurements made in smoke directly over, or within a few kilometers of the fire, that is, in initial smoke. As smoke ages, species within it are removed and others are generated by chemical and physical processes. Various effects of the aging of smoke are discussed by *Hobbs et al.* [2003], *Yokelson et al.* [2003], *Magi and Hobbs* [2003], *Gao et al.* [2003], *Li et al.* [2003], and *Pósfai et al.* [2003].

[37] As mentioned previously, if the correlation coefficient (r^2) for the excess molar mixing ratio of a species against the excess molar mixing ratio of CO (or CO_2) was $\geq$0.5, biomass burning was considered to be a significant source of that species. The emission factors for all such species from the present study are given in Table 4.

[38] Figure 4 shows the EF of several gases plotted against the modified combustion efficiency (MCE) based on gas chromatography analysis of the sixteen canister samples obtained in the 10 fires reported here. The slope of the regression of EF versus MCE indicates the importance of the combustion processes (flaming or smoldering) in determining the emission factor: the steeper the slope, the greater the dependence on the combustion process. A positive slope indicates that emission of the species is favored by flaming combustion (Figure 4a), and a negative slope that it is favored by smoldering combustion (Figures 4b–4f). The effectiveness of the MCE as an independent variable for determining EF is given by the correlation coefficient between EF and MCE. For species that have a high correlation coefficient between EF and MCE, measurements of CO and CO_2 alone (which together determine the MCE) may be used to estimate EF. Similar plots to Figure 4, but for the oxygenated compounds measured by the AFTIR, are given by *Yokelson et al.* [2003].

[39] Table 5 lists slopes, intercepts, and correlation coefficients for the emission factors regressed against MCE for various species collected in the stainless steel canisters and by AFTIR. For many of the species listed in Table 5 (except CO_2 of course, see equation (5)), the emission factor decreases with increasing MCE (indicated by negative slopes in Table 5). This shows that these species are preferentially released during smoldering combustion. However, for those species whose emission factors are weakly correlated with MCE (indicated by low values of r^2 in Table 5), the emissions are not strongly dependent on the combustion process. Our results for SO_2 show a negative slope for EF versus MCE and a reasonably high r^2 value (0.56, Table 5), even though laboratory studies indicate that SO_2 is preferentially released in flaming combustion [*Crutzen and Andreae*, 1990; *Yokelson et al.*, 1996]. This could result from fires with low values of the MCE occurring by chance in fuels with high sulfur content.

[40] Figure 5 compares the emission factors of CO_2, CO, CH_4, and NMOC reported here for the burning of savanna in southern Africa with those reported by *Ferek et al.* [1998] for the burning of grassland in Brazil, and with the global compilation of emission factors for savanna burning by *Andreae and Merlet* [2001]. Taking into account the stand-

Table 4. Emission Factors of Species in Initial Smoke From Savanna Fires in Southern Africa Measured in This Study[a]

Species	Skukuza 1	Skukuza 2	Madikwe 1	Madikwe 2	Madikwe 3	Kruger National Park	Beira	Kaoma 1	Kaoma 2	Timbavati	Average Value ± Standard Deviation From This Study	Average Value ± Standard Deviation [*Andreae and Merlet*, 2001]
Carbon dioxide (CO_2)	1692	1789	1611	1770	1681	1616	1686	1705	1759	1690	1700 ± 60	1613 ± 95
Carbon monoxide (CO)	71	24	120	23	82	97	73	73	42	76	68 ± 30	65 ± 20
Methane (CH_4)	3.0	0.6	3.3	0.8	1.7	2.5	1.1	1.4	0.5	1.8	1.70 ± 0.98	2.3 ± 0.9
Non-methane hydrocarbons compounds (NMHC)	3.4	0.7	4.2	3.7	3.0	8.9	4.4	1.7	1.1	2.9	3.4 ± 2.3	3.4 ± 1.0
Nitrogen Oxides (as NO)	2.9	–	4.1	3.8	–	3.5	3.4	3.5	2.4	2.8	3.3 ± 0.6[b]	3.9 ± 2.4
Sulfur dioxide (SO_2)	–	–	–	–	–	0.87	0.33	0.22	0.30	–	0.43 ± 0.30	0.35 ± 0.16
Dimethyl sulfide (C_2H_6S)	0.0036	0.00048	–	–	0.0013	0.0012	0.0018	0.00049	0.00016	0.0017	0.0013 ± 0.0011	–
Methyl bromide (CH_3Br)	0.0015	0.00027	0.0025	0.00091	0.0010	0.0015	0.00040	0.00048	0.00010	0.0016	0.0010 ± 0.0008	0.0021 ± 0.0010
Methyl chloride (CH_3Cl)	0.18	0.021	0.063	0.081	0.085	0.096	0.033	0.029	0.020	0.10	0.070 ± 0.048	0.075 ± 0.029
Methyl iodide (CH_3I)	0.00081	0.00014	0.00085	–	–	0.0010	0.00055	0.000084	0.000055	0.00058	0.00045 ± 0.00039	0.0005 ± 0.0002
Methyl nitrate (CH_3ONO_2)	0.00019	0.00011	0.0012	0.00079	0.00083	0.00026	0.00040	0.00028	0.00023	0.00075	0.00051 ± 0.00037	–
Ethane (C_2H_6)	0.42	0.08	0.29	0.13	0.25	0.33	0.096	0.19	0.078	0.25	0.21 ± 0.12	0.32 ± 0.16
Ethene (C_2H_4)	0.83	0.27	1.1	0.21	0.90	0.77	0.78	0.43	0.38	0.73	0.64 ± 0.30	0.79 ± 0.56
Propane (C_3H_8)	0.14	0.020	0.088	0.029	0.056	0.086	0.0014	0.048	0.016	0.064	0.054 ± 0.041	0.09 ± 0.03
Propene (C_3H_6)	0.35	0.11	0.51	0.070	0.29	0.31	0.11	0.17	0.10	0.27	0.23 ± 0.14	0.26 ± 0.14
Acetylene (C_2H_2)	0.28	0.063	0.27	0.097	0.30	0.29	0.35	0.16	0.16	0.23	0.220 ± 0.095	0.29 ± 0.27
i-butane (C_4H_{10})	0.012	0.0016	0.0092	0.0028	0.0051	0.0072	0.0007	0.0040	0.0010	0.0067	0.0050 ± 0.0037	0.006 ± 0.003
n-butane (C_4H_{10})	0.032	0.0047	0.029	0.0076	0.014	0.022	–	0.013	0.0048	0.018	0.016 ± 0.010	0.019 ± 0.090
t-2-butene (C_4H_8)	0.023	0.0063	0.027	0.0023	0.015	0.022	0.0096	0.010	0.0038	0.016	0.013 ± 0.009	0.024 ± 0.014
1-butene (C_4H_8)	0.067	0.021	0.090	0.012	0.057	0.057	0.0052	0.034	0.019	0.050	0.041 ± 0.027	0.09 ± 0.06
c-2-butene (C_4H_8)	0.017	0.0046	0.0202	0.0020	0.011	0.0160	0.0042	0.0072	0.0028	0.012	0.0097 ± 0.0065	0.021 ± 0.011
n-pentane (C_5H_{12})	–	0.00060	0.0106	0.0021	0.0045	0.0069	–	0.0041	0.0019	0.0050	0.0045 ± 0.0032	0.005 ± 0.004
1, 3-butadiene (C_4H_6)	0.066	0.023	0.11	0.011	0.067	0.067	0.055	0.039	0.027	0.055	0.052 ± 0.028	0.07 ± 0.05
3-methyl-1-butene (C_5H_{10})	0.0089	0.0026	0.012	0.0013	0.0066	0.0064	0.0016	0.0038	0.0022	0.0063	0.0051 ± 0.0034	–
t-2-pentene (C_5H_{10})	0.0085	0.0021	0.0081	0.0004	0.0050	0.0073	0.0032	0.0033	0.0015	0.0052	0.0045 ± 0.0028	–
2-methyl-2-butene (C_5H_{10})	0.010	0.0017	0.0090	0.00031	0.0046	0.0087	0.0029	0.0040	0.0013	0.0058	0.0048 ± 0.0035	0.008 ± 0.004
2-methyl-1-butene (C_5H_{10})	0.010	0.0021	0.011	–	–	0.0083	0.0028	0.0044	0.0016	0.0066	0.0059 ± 0.0037	0.008 ± 0.004
c-2-pentene (C_5H_{10})	0.0045	0.0014	0.0047	–	–	0.0043	0.0012	0.0019	0.00094	0.0032	0.0025 ± 0.0018	–
n-hexane (C_6H_{14})	–	0.0033	0.0284	–	0.013	0.0155	0.0126	0.0101	0.0071	0.0133	0.013 ± 0.0074	0.039 ± 0.045
Isoprene (C_5H_8)	0.077	0.011	0.069	0.0095	0.031	0.037	0.055	0.053	0.036	0.037	0.042 ± 0.022	0.02 ± 0.012
2-methyl-1-pentene (C_6H_{12})	0.0049	0.0020	0.0077	–	0.0029	0.0040	0.0029	0.0028	0.0003	0.0043	0.0035 ± 0.0021	–
n-heptane (C_7H_{16})	–	0.00015	0.023	–	0.0014	0.0090	0.0058	0.0056	0.0040	0.0065	0.0070 ± 0.0072	–
Benzene (C_6H_6)	0.26	0.069	0.28	0.047	0.22	0.25	0.23	0.13	0.089	0.20	0.18 ± 0.09	0.23 ± 0.11
Toluene (C_7H_8)	0.017	0.00056	0.33	0.06	0.19	0.0057	0.17	0.15	0.11	0.067	0.13 ± 0.10	0.13 ± 0.06
Formaldehyde (HCHO)	1.4	1.4	0.96	1.2	1.2	0.87	1.4	0.75	0.39	1.5	1.1 ± 0.38	0.26–0.44
Methanol (CH_3OH)	1.4	1.4	1.2	0.86	0.86	1.8	1.6	1.0	0.32	1.2	1.20 ± 0.46	1.3
Acetic acid (CH_3CO_2H)	3.4	3.4	2.3	1.8	1.8	2.8	3.6	2.2	0.80	2.3	2.4 ± 0.89	1.3
Formic acid (HCO_2H)	0.29	0.29	0.70	0.73	0.73	0.69	0.76	0.57	0.43	0.79	0.62 ± 0.18	0.7

Table 4. (continued)

Species	Skukuza 1	Skukuza 2	Madikwe 1	Madikwe 2	Madikwe 3	Kruger National Park	Beira	Kaoma 1	Kaoma 2	Timbavati	Average Value ± Standard Deviation From This Study	Average Value ± Standard Deviation [*Andreae and Merlet*, 2001]
Ammonia (NH_3)	0.39	0.39	0.32	0.38	0.38	0.13	–	0.40	–	0.070	0.26 ± 0.14	0.6 –1.05
Hydrogen cyanide (HCN)	0.76	0.76	0.67	0.64	0.64	0.44	0.55	0.37	0.31	0.52	0.53 ± 0.15	0.028
Total particulate matter (TPM)[c]	11	1.7	–	3.5	14	–	–	13	4.8	23	10.0 ± 7.5	8.3 ± 3.2
Organic particulate carbon (OC)	3.5	0.68	–	1.3	3.3	2.2	1.7	3.0	0.70	4.0	2.3 ± 1.2	3.4 ± 1.4
Black carbon (BC)	0.45	0.081	–	–	0.63	0.41	0.25	0.47	0.24	0.68	0.39 ± 0.19	0.48 ± 0.18
Total particulate carbon (TC)	4.0	0.76	–	1.6	3.9	2.6	2.0	3.5	0.94	4.7	2.7 ± 1.4	3.7 ± 1.3
Chloride (Cl^-)	0.57	0.18	–	0.087	1.9	–	–	0.26	0.0093	3.8	0.97 ± 1.40	–
Nitrate (NO_3^-)	0.099	0.013	–	0.25	0.29	–	–	0.19	0.050	0.26	0.16 ± 0.11	–
Sulfate (SO_4^{2-})	0.027	0.003	–	–	0.26	–	–	0.14	0.09	0.48	0.17 ± 0.18	–
Potassium (K^+)	0.17	0.092	–	0.22	–	–	–	0.38	0.12	1.4	0.50 ± 0.53	0.34 ± 0.15
Condensation nuclei (CN)	–	–	–	–	–	2.0×10^{16}	2.7×10^{16}	5.9×10^{16}	1.7×10^{16}		$(3.0 \pm 1.7) \times 10^{16}$	3.4×10^{15}
Particles 0.1–3.0 μm diameter ($CN_{0.1-3\ \mu m}$)	5.3×10^{14}	1.8×10^{13}	–	2.4×10^{14}	8.9×10^{13}	2.7×10^{14}	1.6×10^{14}	2.1×10^{14}	1.5×10^{14}		$(2.0 \pm 1.5) \times 10^{14}$	–

[a] Also listed are the corresponding values given by *Andreae and Merlet* [2001] for savanna and grassland burning. Emission factors have units of grams of species emitted per kilogram of fuel burned, except for CN and $CN_{0.1-3\ \mu m}$, which have units of number of particles emitted per kilogram of fuel burned. See Table 1 for information on each fire and Tables 2 and 3 for techniques used for measurements. When emission factors were measured by both GC/C and AFTIR, the GC/C values are given here. See Figure 8 for comparison of the two techniques.

[b] The average value of the molar ratio NO/NO_2 was 0.58 ± 0.15.

[c] For particles up to ~4 μm diameter.

ard deviations of the measurements, the mean emission factors for CO_2, CO, CH_4, and NMHC provided by these three studies are similar.

[41] Figure 6 compares the emission factors reported here for total particulate matter, total particulate carbon, organic carbon, and black carbon with those given by *Ferek et al.* [1998] for the burning of grassland in Brazil and with the compilation by *Andreae and Merlet* [2001]. In view of the standard deviations of the measurements, the mean emission factors for total particulate matter, total carbon, organic carbon, and black carbon given in these three studies are similar.

[42] The single-scattering albedo of smoke emitted from biomass fires depends on the ratio of organic carbon to black carbon [*Mazurek et al.*, 1991]. The ratio of the emission factors of black carbon to organic carbon in this study is 0.17 ± 0.12. The corresponding value given by *Andreae and Merlet* [2001] for savanna and grassland burning is 0.14 ± 0.08.

[43] The emission factors of several compounds reported here (Table 4 and Figure 7) differ from those reported by *Andreae and Merlet* [2001]. For example, the average emission factor for NH_3 measured in this study is 0.26 ± 0.15 g kg^{-1} compared to 0.6–1.5 g kg^{-1} given by Andreae and Merlet. Multiplying the average NH_3 emission factor for savanna fires in southern Africa given here by an estimate for savanna burned in Africa (1600 Tg yr^{-1} [*Hao and Liu*, 1994]) yields 0.34 ± 0.27 Tg yr^{-1} of NH_3 emitted by African savanna fires. Since the emission of ammonia from all sources worldwide is believed to be ~55 Tg yr^{-1} [*Seinfeld and Pandis*, 1998], savanna burning in Africa makes only a small contribution to global NH_3 emissions. Boreal forest fires have a large emission factor for NH_3 and may produce more total NH_3 emissions [*Goode et al.*, 2000].

[44] As mentioned earlier, AFTIR samples obtained in this study showed that oxygenated organic compounds were a major component of smoke from young savanna fires. On a mass basis the oxygenated emissions dominate the organic emissions. The oxygenates have important effects on chemical reactions in a smoke plume, as described by *Mason et al.* [2001]. On a mass basis acetic acid is the major initial organic emission (EF = 2.4 ± 0.9 g/kg), and its concentration rapidly increases downwind [*Hobbs et al.*, 2003; *Yokelson et al.*, 2003]. Methanol and formaldehyde are the other two major oxygenates emitted by these fires. Methanol is a source of HO_2 and HCHO in the atmosphere. The average emission factor for the direct emission of HCHO given here is 1.1 ± 0.38 g kg^{-1} (Table 4), compared to 0.26–0.44 g kg^{-1} given by *Andreae and Merlet* [2001]. Multiplying our average HCHO emission factor for savanna burning by the estimate of 1600 Tg yr^{-1} for savanna burned in Africa, yields ~1.8 ± 0.62 Tg yr^{-1} of HCHO emitted from savanna fires in Africa. Photolysis of HCHO produces HO_2, which leads to conversion of NO to NO_2 and subsequent ozone formation. Therefore, HCHO emissions from savanna burning may lead to increased initial ozone formation rates [*Yokelson et al.*, 1999]. The oxygenated organic compounds were strongly affected by cloud processing [*Yokelson et al.*, 2003].

[45] Our average emission factor for HCN is 0.53 ± 0.15 g kg^{-1} (Table 4), compared to 0.025–0.03 g kg^{-1} given by

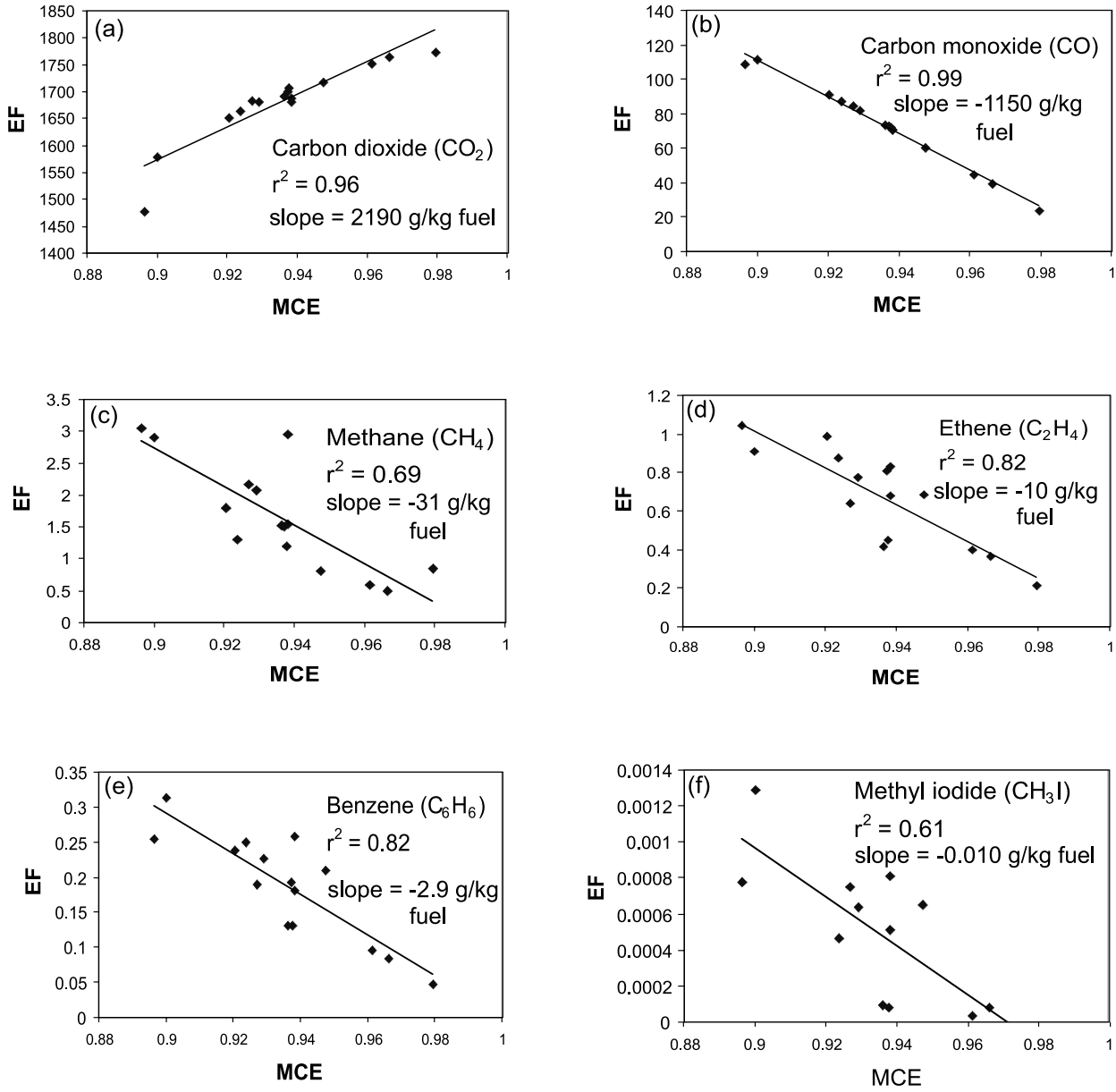

Figure 4. Emission factors (grams of species emitted per kilogram of fuel burned) versus modified combustion efficiency (MCE) for various trace gases in each of sixteen canister samples. The correlation coefficient is given by r^2.

Andreae and Merlet [2001]. Since the major global source for HCN is biomass burning, and since this species can be monitored from space, HCN has been proposed as a tracer for biomass burning [*Li et al.*, 2000]. The abundance of HCN emitted by African savanna fires lends support to this proposal. It should be noted that HCN can interfere with NO_y measurements [*Kliner et al.*, 1997].

[46] The emission factor for aerosols (i.e., Aitken nuclei or condensation nuclei [CN]) given by *Andreae and Merlet* [2001], namely 3.4×10^{15} particles per kilogram of fuel burned, is based on laboratory measurements. Taking into account the uncertainty in the measurements, our CN emission factor for savanna burning in southern Africa is ~3–14 times greater than the value given by Andreae and Merlet (Table 4 and Figure 7). Multiplying our average CN emission factor, $(3.0 \pm 1.7) \times 10^{16}$ particles per kilogram of fuel burned, by Hao and Liu's estimate of 1600 Tg yr^{-1} for savanna burned in Africa, yields 2×10^{28} to 8×10^{28} CN emitted per year from African savanna fires. This estimate is about an order of magnitude greater than an earlier estimate by *Le Canut et al.* [1996] of $\sim 3 \times 10^{27}$ to 8×10^{27} particles emitted per year worldwide by savanna fires. Since ~30–100% of submicron biomass smoke particles can act as cloud condensation nuclei [*Rodgers et al.*, 1991], the particles emitted by African savanna fires could have important effects on cloud microstructures.

Table 5. Average Values of Regression Slopes, Regression Intercepts, and Correlation Coefficients (r^2) for Emission Factors (EF)[a] Versus Modified Combustion Efficiency (MCE) for Initial Smoke From Savanna Fires Sampled in Southern Africa in This Study

Species	Technique Used for Measurement[b]	Slope	Intercept	r^2
Carbon dioxide (CO_2)	GC/C	2190	−357	0.96
Carbon monoxide (CO)	GC/C	−1150	1150	0.99
Methane (CH_4)	GC/C	−31	31	0.69
Nonmethane organic compounds (NMOC)	GC/C	−50	50	0.33
Nitrogen oxides (as NO)	AFTIR	−5.8	8.7	0.04
Sulfur dioxide (SO_2)	Teco 43S (via "grab bag")	−11	10	0.56
Dimethyl sulfide (CH_3SCH_3)	GC/C	−0.020	0.021	0.16
Methyl bromide (CH_3Br)	GC/C	−0.020	0.020	0.54
Methyl chloride (CH_3Cl)	GC/C	−0.52	0.56	0.08
Methyl iodide (CH_3I)	GC/C	−0.010	0.011	0.61
Methyl nitrate (CH_3ONO_2)	GC/C	−0.006	0.006	0.18
Ethane (C_2H_6)	GC/C	−2.9	2.9	0.44
Ethene (C_2H_4)	GC/C	−10	10	0.82
Propane (C_3H_8)	GC/C	−0.87	0.87	0.31
Propene (C_3H_6)	GC/C	−4.5	4.4	0.72
Acetylene (C_2H_2)	GC/C	−2.8	2.8	0.62
i-butane (*i*-C_4H_{10})	GC/C	−0.090	0.087	0.39
n-butane (*n*-C_4H_{10})	GC/C	−0.28	0.28	0.62
t-2-butene (C_4H_8)	GC/C	−0.28	0.28	0.77
1-butene (C_4H_8)	GC/C	−0.80	0.79	0.61
c-2-butene (C_4H_8)	GC/C	−0.20	0.20	0.70
i-pentane (*i*-C_5H_{12})	GC/C	−0.03	0.03	0.86
n-pentane (*n*-C_5H_{12})	GC/C	−0.10	0.098	0.89
1, 3-butadiene (C_4H_6)	GC/C	−1.0	0.99	0.88
3-methyl-1-butene (C_5H_{10})	GC/C	−0.10	0.10	0.62
t-2-pentene (C_5H_{10})	GC/C	−0.090	0.087	0.69
2-methyl-2-butene (C_5H_{10})	GC/C	−0.10	0.10	0.66
2-methyl-1-butene (C_5H_{10})	GC/C	−0.11	0.11	0.65
c-2-pentene (C_5H_{10})	GC/C	−0.050	0.047	0.58
n-hexane (C_6H_{14})	GC/C	−0.26	0.26	0.86
Isoprene (C_5H_8)	GC/C	−0.57	0.58	0.47
2-methyl-1-pentene (C_6H_{12})	GC/C	−0.07	0.68	0.65
n-heptane (C_7H_{16})	GC/C	−0.21	0.21	0.61
Benzene (C_6H_6)	GC/C	−2.9	2.9	0.82
Toluene (C_7H_8)	GC/C	−2.1	2.1	0.31
Formaldehyde (HCHO)	AFTIR	−13.94	19.17	0.48
Methanol (CH_3OH)	AFTIR	−21.28	21.17	0.80
Acetic acid (CH_3CO_2H)	AFTIR	−45.33	45.03	0.93
Formic acid (HCO_2H)	AFTIR	−7.51	7.77	0.15
Ammonia (NH_3)	AFTIR	−3.71	3.75	0.12
Hydrogen cyanide (HCN)	AFTIR	−3.07	3.42	0.15
Total particulate matter (TPM)	F/BH	−292	288	0.75
Total carbon (TC)	F/BH	−43	43	0.49
Organic carbon (OC)	F/GB	−37	38	0.47
Black carbon (BC)	F/GB	−5.8	5.8	0.47
Chloride (Cl^-)	F/GB	−39	38	0.38
Nitrate (NO_3^-)	F/GB	−2.4	2.5	0.24
Sulfate (SO_4^{2-})	F/GB	−5.4	5.3	0.39
Potassium (K^+)	F/GB	−16	16	0.45

[a]Emission factors are expressed as grams per kilogram of fuel burned.
[b]GC/C = gas chromatography via canister; F/GB = filters via grab bag; AFTIR = Airborne Fourier Transform Infrared spectroscopy.

[47] Table 4 lists emission factors for eleven species that do not appear in the compilation of emission factors for biomass burning given by *Andreae and Merlet* [2001]. These species are DMS, methyl nitrate, five hydrocarbons (3-methyl-1-butene, *c*-2-pentene, *t*-2-pentene, 2-methyl-1-pentene, and *n*-heptane), the particulate anions Cl^-, SO_4^{2-} and NO_3^-, and particles in the size range 0.1 to 3 μm diameter ($CN_{0.1-3\ \mu m}$). For all these species, the correlation coefficient (r^2) of the excess mixing ratio versus the excess mixing ratio of CO was $\geq$0.5, indicating that they were emitted by biomass burning. Except for Cl^-, SO_4^{2-} and NO_3^-, these species have not been previously reported for biomass burning of savanna in southern Africa. These species are discussed in turn below.

[48] The oxidation of DMS to SO_2 can lead subsequently to the formation of sulfate particles. Average emission factors for DMS, SO_2 and SO_4^{2-} from this study are, respectively, 0.0013 ± 0.001, 0.43 ± 0.30, and 0.17 ± 0.18 grams per kilogram of fuel burned (Table 4). The large standard deviations in these values reflect the high variability in the emissions of these species, which is not surprising since fuel sulfur content varies greatly. Nevertheless, the average value of the emission factor for DMS is about a factor of 100 below that of SO_2 and SO_4^{2-}. There-

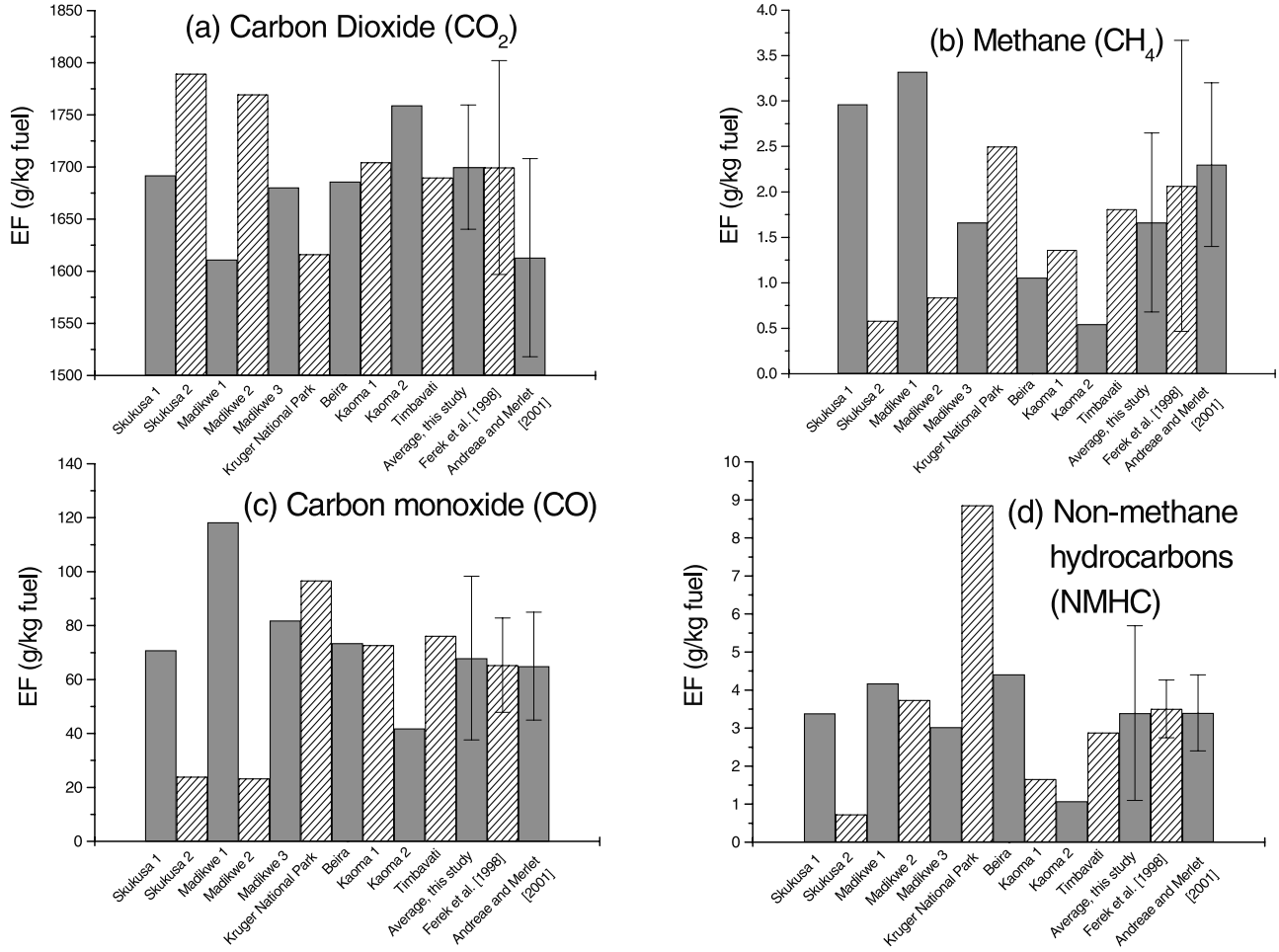

Figure 5. Emission factors (EF) for CO_2, CO, CH_4, and NMHC, derived from canister measurements, for the burning of savanna in southern Africa (this study), grassland in Brazil [*Ferek et al.*, 1998], and global savanna burning [*Andreae and Merlet*, 2001].

fore, on average, the direct emission of SO_4^{2-} from the fires probably dominated over the subsequent production of SO_4^{2-} through DMS oxidation, but not over SO_4^{2-} production due to the oxidation of SO_2 emitted directly from the fires.

[49] Methyl nitrate (CH_3ONO_2) can serve to redistribute NO_2 in regions distant from its source, which can then lead to O_3 formation [*Warneck*, 2000]. The average emission factor for CH_3ONO_2 measured in this study of young smoke is only 0.00051 ± 0.00037 grams per kilogram of fuel burned, compared to 3.3 ± 0.6 g kg^{-1} for NO_x as NO (Table 4). However, CH_3ONO_2 and NO_x could have comparable mixing ratios in older smoke.

[50] The five new hydrocarbons we detected in the smoke over the fires are reactive alkanes and alkenes. Because the OH radical is a major oxidant for these five hydrocarbons, their presence will reduce the concentration of OH, and therefore oxidation by OH, downwind in smoke plumes. All five hydrocarbons decreased significantly as the smoke aged [*Hobbs et al.*, 2003].

[51] The emission factors for Cl^-, SO_4^{2-} and NO_3^- reported here, namely, 0.97 ± 1.4, 0.16 ± 0.11 and 0.17 ± 0.18 g kg^{-1}, respectively, can be compared with the corresponding values given for savanna, forest and agricultural fires in southern Africa by *Andreae et al.* [1998], namely, 1.40 ± 0.35, 0.37 ± 0.20 and 0.59 ± 0.24, respectively. The values given by Andreae et al. may be larger because of higher nutrient content in agricultural fuels and/or because they sampled older smoke than we did.

[52] Emission factors for the particulate ionic species can be compared to their most abundant corresponding gaseous species. For example, the molar ratio of the emission factors of NO_3^- to NO_x is 0.022, and the molar ratio of the emission factors of SO_4^{2-} to SO_2 is 0.26. These ratios indicate that most of the nitrogen released from the fires was in gaseous form as NO_x, and about four times as much SO_2 was released as was SO_4^{2-}. Furthermore, chemical transformations from NO_x to nitrate, and from SO_2 to sulfate, could have occurred even in the initial smoke. However, the latter transformation must have occurred more rapidly than the former. The molar ratio of the emission factor of Cl^- to CH_3Cl is 20, which suggests that most of the chlorine released was in particulate form as Cl^-.

[53] The emission factors for Cl^-, NO_3^- and SO_3^{2-} can be compared with those for K^+ and NH_3, to check the balance between emissions of positive and negative ions. The emission factors for K^+ and Cl^- are 0.50 ± 0.53 and 0.97 ± 1.4 g kg^{-1} (or 0.013 ± 0.014 and 0.027 ± 0.039 mol

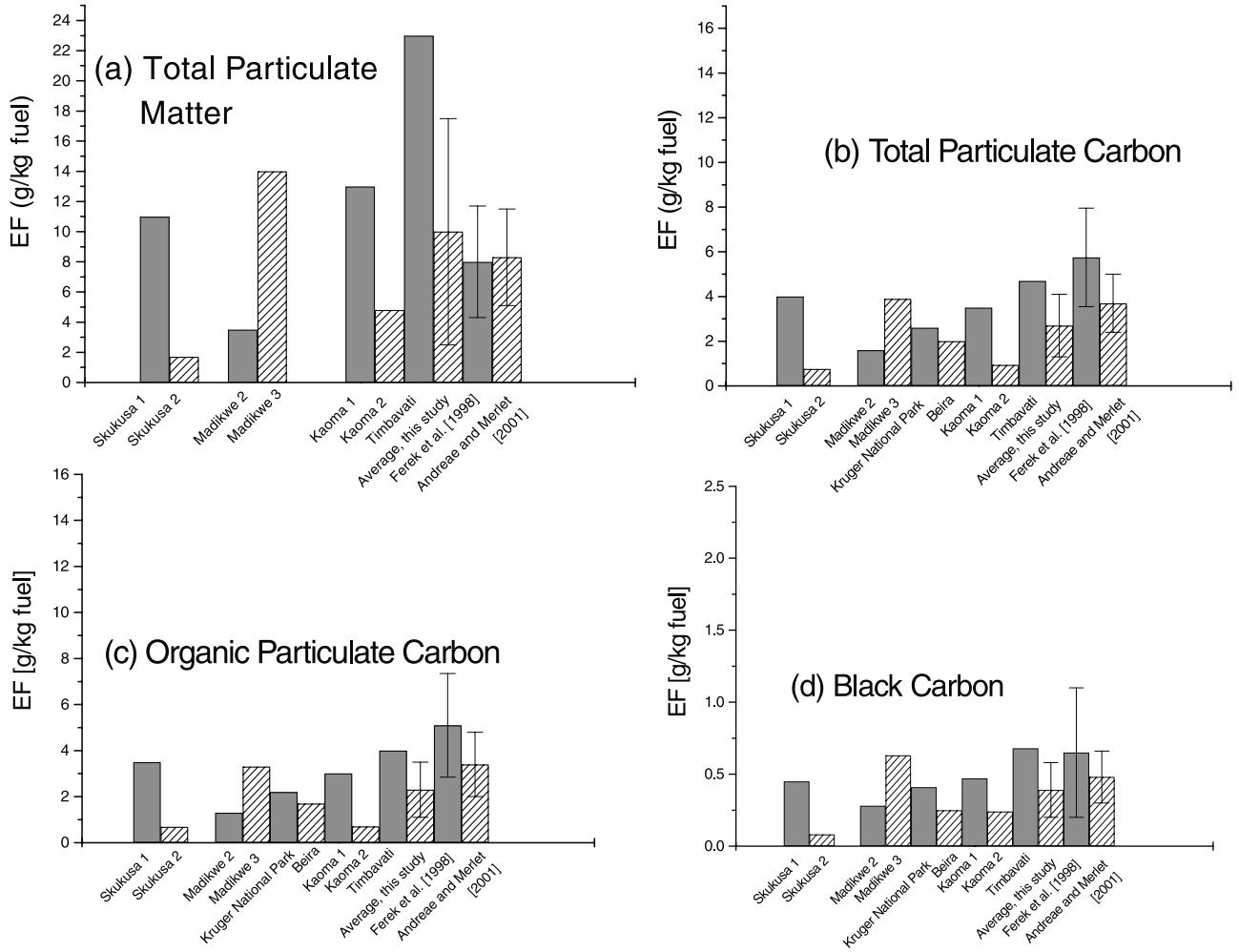

Figure 6. As for Figure 5 but for total particulate matter, total particulate carbon, organic particulate carbon and black carbon.

kg^{-1}), respectively, which are not significantly different (K^+ and Cl^- can form the neutral KCl). Ammonia is the primary basic gas in the atmosphere, which can neutralize HNO_3 and H_2SO_4. The emission factor for NH_3 is 0.26 ± 0.15 g kg^{-1} (or 0.015 ± 0.009 mol kg^{-1}), while the sum of the emission factors for NO_3^- and SO_4^{2-} is 0.33 ± 0.21 g kg^{-1} (or 0.0044 ± 0.0026 mol kg^{-1}). These comparisons indicate that, on average and within the variability of the measurements, the positive and negative ions emitted by the fires were in charge balance.

[54] Aerosol surface area is one of the main factors that determines the rates of heterogeneous reactions, and most of the surface area of aerosols in the atmosphere is associated with accumulation mode particles, which have peak concentrations at a diameter of about 0.1 μm. Also, since accumulation mode particles are not removed very efficiently from the atmosphere, they have relatively long residence times [e.g., *Hobbs*, 2000]. As shown in Table 4, the average emission factor of particles with diameters from 0.1 to 3 μm (i.e., accumulation-mode particles) from savanna burning in southern Africa measured in this study was $(2.0 \pm 1.5) \times 10^{14}$ particles per kilogram of fuel burned, compared to $(3.0 \pm 1.7) \times 10^{16}$ total (CN) particles emitted per kilogram of fuel burned. If it is assumed that all particles in the accumulation mode have a diameter of 0.1 μm, the emission factor for the surface area of these particles is (6.3 ± 4.7) m^2 per kilogram of fuel.

[55] Based on the $CN_{0.1-3\ \mu m}$ and CN emission factors, only ~1% by number of the particles in the initial smoke were in the accumulation mode. Particle size spectra measured with the DMPS showed that the particle mode diameter in the initial smoke was ~0.01 μm, with most of the particles ranging from ~0.01–0.03 μm. As smoke ages, particle coagulation and gas-to-particle conversion increase the particle mode diameter [*Hobbs et al.*, 2003].

6. Comparisons of Measurements Using Gas Chromatography and Fourier Transform Infrared Spectroscopy

[56] In laboratory studies, *Goode et al.* [1999] obtained excellent agreement for the concentrations of a number of gaseous species measured in the same biomass smoke by gas chromatography on canister samples (GC/C) and by Fourier transform infrared spectroscopy. In the field studies described in the present paper, five species (CO_2, CO, CH_4, C_2H_2 and C_2H_4) were measured by both GC/C and by AFTIR. This provides a unique opportunity to compare

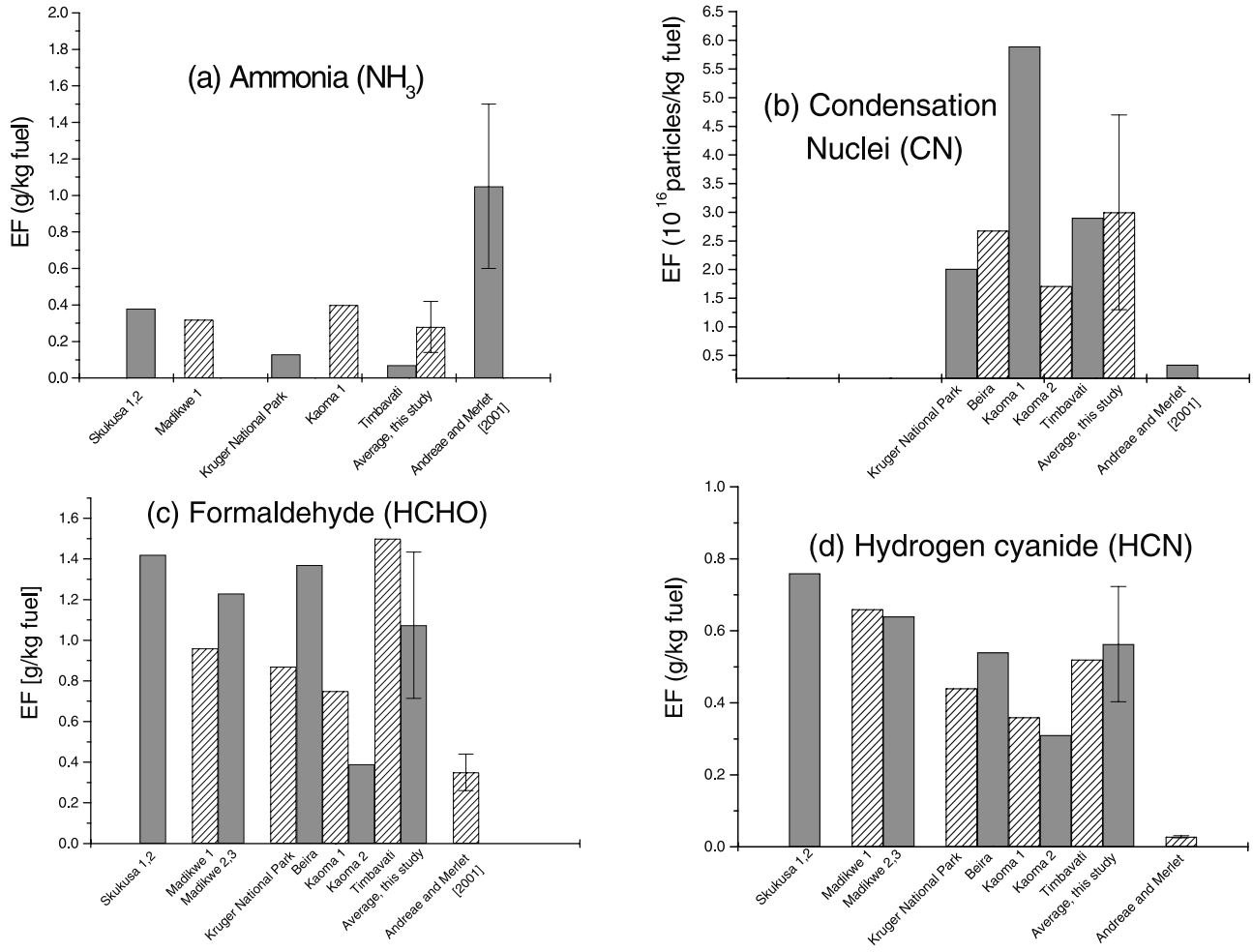

Figure 7. Emission factors (EF) for ammonia, condensation nuclei, formaldehyde, and hydrogen cyanide from the burning of savanna in southern Africa measured in this study compared to those given for global savanna burning by *Andreae and Merlet* [2001].

measurements from these two independent techniques under field conditions. However, in doing so it should be pointed out that in the present study the GC/C and AFTIR measurements were not made on exactly the same smoke samples. Also, whereas a single ambient GC/C sample was obtained for each fire, multiple ambient AFTIR measurements were obtained.

[57] Shown in Table 6 are comparisons of both emission factors and MCEs derived from the GC/C and AFTIR measurements for the 10 fires described in this paper. The emission factors derived from these two independent measuring techniques are in good agreement for the Madikwe 2, 3, Kruger National Park, Kaoma 1, and Kaoma 2, and the Timbavati fires. For these fires, the MCE derived from the GC/C and AFTIR measurements are either identical or similar, indicating that similar smoke was sampled by both techniques. For the Skukuza 1, 2 and Beria fires, the smoke sampled for the GC/C measurements had higher average MCEs than the smoke sampled by the AFTIR. Consistent with this, the emission factor for CO_2 was greater, and the emission factors for the smoldering products (CO, CH_4, C_2H_2 and C_2H_4) were lower from the GC/C measurements than from the AFTIR. The reverse was true for the Madikwe 1 fire, where the smoke sampled for the GC/C measurements had a lower MCE than the smoke sampled by the AFTIR. We conclude from these results that the GC/C and AFTIR provided similar results when they sampled similar smoke.

[58] Comparisons of study-average emission ratios and emission factors for CO_2, CO, CH_4, C_2H_2 and C_2H_4 derived from the GC/C and AFTIR are shown in Figure 8. The values obtained from the two techniques are in good agreement, with the exception of C_2H_4 (ethene). The average emission ratios for C_2H_4 from GC/C and AFTIR are 0.0110 ± 0.0005 and 0.017 ± 0.003, respectively. *Ferek et al.* [1998] reported a C_2H_4 emission ratio of 0.011 obtained by GC/C for young smoke from grass, cerrado, and forest fires in Brazil. *Blake et al.* [1996] reported C_2H_4 emission ratios from GC/C of 0.0083 ± 0.0006 and 0.0061 ± 0.0004 for young and aged smoke (with depleted C_2H_4) from savanna fires in southern Africa and from agricultural fires in Brazil, respectively. Hence, the C_2H_4 emission ratios measured by several workers using GC/C are lower in magnitude than those obtained in this study using AFTIR, although this was not the case in the work of *Goode et al.* [1999].

Table 6. Modified Combustion Efficiency (MCE) and Emission Factors[a] Measured by Gas Chromatography on Canister Samples (GC/C) and by Airborne Fourier Transform Infrared Spectroscopy (AFTIR)[b]

Measurement	Technique Used for Measurement	Skukuza 1, 2[c]	Madikwe 1	Madikwe 2, 3[c]	Kruger National Park	Beira	Kaoma 1	Kaoma 2	Timbavati	Study Average
MCE	GC/C	0.96	0.90	0.96	0.93	0.95	0.94	0.96	0.94	0.94 ± 0.02
	AFTIR	0.93	0.94	0.96	0.93	0.91	0.94	0.97	0.94	0.94 ± 0.02
Emission factor										
Carbon dioxide	GC/C	1741	1611	1726	1616	1686	1705	1759	1690	1700 ± 51
	AFTIR	1678	1715	1738	1688	1643	1711	1779	1696	1706 ± 38
Carbon monoxide	GC/C	48	120	53	97	73	73	42	76	68 ± 24
	AFTIR	84	64	51	78	103	69	30	75	69 ± 21
Methane	GC/C	1.8	3.3	1.3	2.5	1.1	1.4	0.5	1.8	1.7 ± 0.8
	AFTIR	2.8	2.0	1.4	3.1	3.6	1.4	0.6	2.5	2.2 ± 0.9
Ethene	GC/C	0.55	1.1	0.56	0.77	0.78	0.43	0.38	0.73	0.64 ± 0.22
	AFTIR	1.61	0.97	1.02	1.22	1.60	0.82	0.69	1.19	1.14 ± 0.31
Acetylene	GC/C	0.17	0.27	0.20	0.29	0.35	0.16	0.16	0.23	0.22 ± 0.07
	AFTIR	0.26	0.22	0.26	0.31	0.36	0.24	0.20	0.24	0.26 ± 0.05

[a]Emission factors expressed as grams of species emitted per kilogram of fuel burned.
[b]A total of 16 GC/C samples and 36 AFTIR samples were obtained for the 10 fires listed.
[c]Measurements for Skukuza 1 and 2 are averaged together since they were obtained on similar fires located close together on the same day; similarly for Madikwe 2 and 3.

[59] The study-average emission factors for C_2H_4 from the GC/C and AFTIR are 0.64 ± 0.22 and 1.14 ± 0.31 grams per kilogram of fuel burned, respectively. If these two average values are weighted by the number of samples obtained for the GC/C and AFTIR measurements (16 and 36, respectively), and then combined to yield an overall study-average for the emission factor of C_2H_4, the value obtained is 0.99 ± 0.28 grams per kilogram of fuel burned. *Andreae and Merlet* [2001] give a value of (0.79 ± 0.56) g/kg for the emission factor of C_2H_4 from savanna and grassland fires.

7. Emission Fluxes

[60] Table 7 provides estimates of emission fluxes for those species that have not been reported previously as emissions from African savanna fires and those for which the emission factors given in this paper differ significantly from previously published values. The emission fluxes were estimated by multiplying the study-average emission factors given in Table 4 by estimates of the total amount of savanna burned in Africa and worldwide. For African savanna fires we used the estimate of 1600 Tg yr^{-1} reported by *Hao and Liu* [1994], and for savanna fires worldwide we used an estimate of 1410 Tg (C) yr^{-1} [*Lobert et al.*, 1999], or assuming a carbon content for savanna fuels of 50%, 2820 Tg fuel yr^{-1}.

[61] In the case of DMS, ammonia and formaldehyde, emissions from savanna fires are minor in comparison to total global sources. However, emissions from African and global savanna fires contribute ~40% and ~70%, respectively, of the global emissions of HCN. Total global sources of the other species listed in Table 7 are unknown.

[62] The emission fluxes for savanna fires given in Table 7 are based on the study-average emission factors given in this paper. However, Table 4 provides emission factors for 10 fires covering various savanna types, including the lowveld and bushveld dry savanna biomes and the miombo and dambo humid savanna biomes. *Hao and Liu* [1994] provide the spatial distribution of African savanna burning with a resolution of 5° latitude by 5° longitude for the fourth month of the burning season during the late 1970s. For the 5° by 5° cell covering southern Congo, which is a region of predominantly miombo woodland, Hao and Liu estimated that 9 Tg of savanna were burned in that month. To estimate emissions of a species from southern Congo during that month, the appropriate emission factor from the Kaoma 1 fire (Table 4) could be used since this fire occurred in miombo woodland. Using vegetation-specific emission factors for all the months of the burning season in Africa would yield more accurate annual flux estimates than those given in Table 7. However, such estimates require a spatially and temporally resolved database for the quantity and type of savanna burned throughout Africa over the entire burning season.

8. Summary and Conclusions

[63] In this paper we have reported emission ratios and emission factors for 50 species in initial smoke from savanna fires in southern Africa. Apart from CN and $CN_{0.1-3\ \mu m}$, the emission factors for all these species are summarized in Figure 9. The correlation coefficients (r^2) of the excess mixing ratio of these species versus the excess mixing ratio of CO or CO_2 were all $\geq$0.5; accordingly, these species were considered to be emitted by the fires. The fuels burned in the fires sampled represent vegetation types from the lowveld to the highveld in South Africa, to dambo and miombo woodlands in Zambia, to east African coastal mosaic in Mozambique (Table 1).

[64] For most species, there is good agreement between the emission ratios and emission factors reported here for initial smoke from savanna fires in southern Africa and those given by *Ferek et al.* [1998] for initial smoke from fires in Brazil and (for stable compounds) by *Blake et al.* [1996] for mainly aged smoke from savanna fires in southern Africa, as well as with a recent compilation of measured and estimated emission factors for savanna burning worldwide by *Andreae and Merlet* [2001]. However, this study provides the first measurements of numerous species in initial smoke from savanna fires in southern Africa, and the first measurements for eight species that have not been reported previously. In some cases, the emission ratios and emission factors given here differ significantly from the

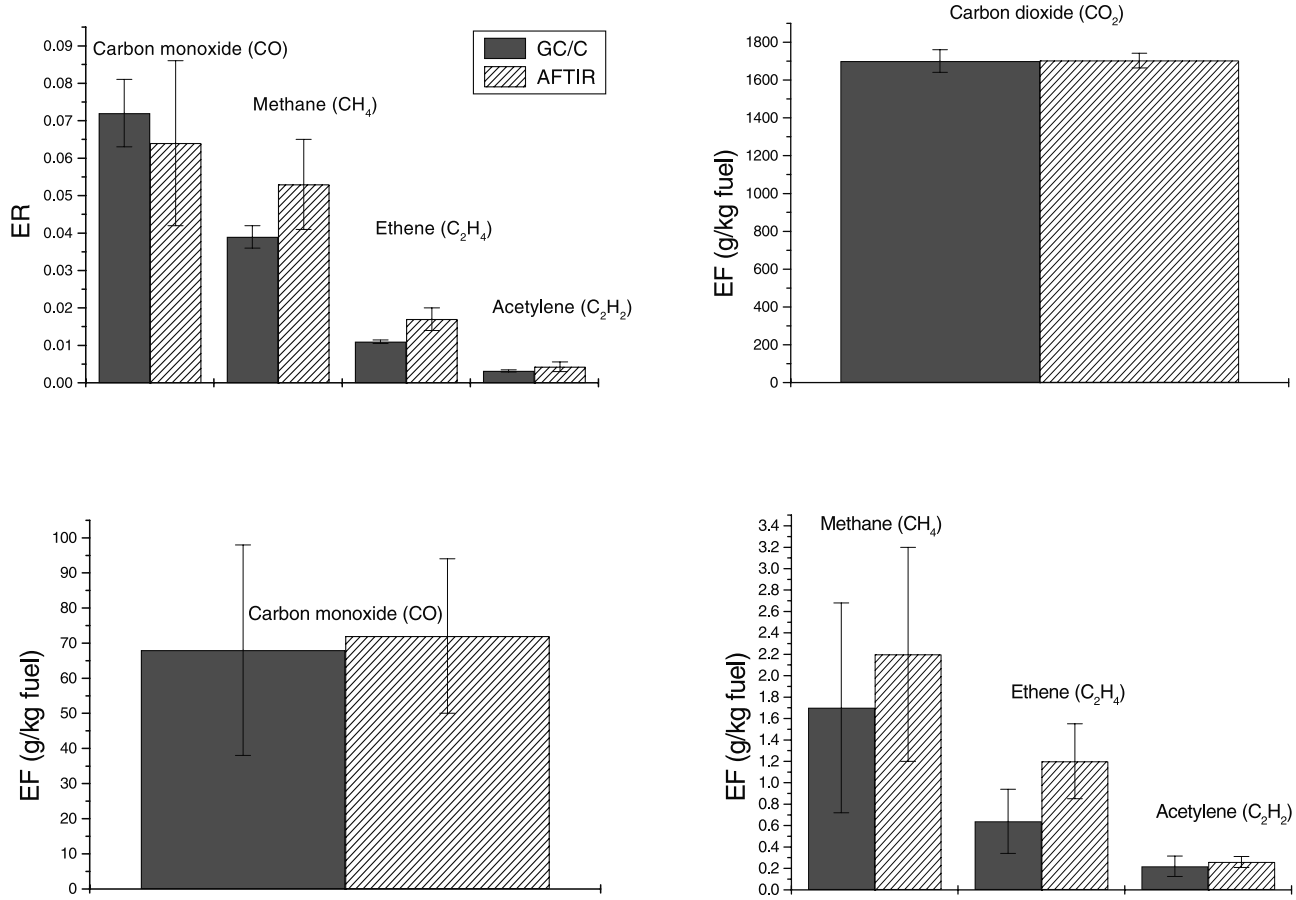

Figure 8. Comparisons of molar emission ratios (ER) and emission factors (EF) for savanna fires in southern Africa for carbon monoxide (with respect to CO_2) and methane, ethane and acetylene (with respect to CO), and emission factors for carbon dioxide, carbon monoxide, methane, ethane and acetylene, calculated from two independent measurement techniques: gas chromatography on canister samples and AFTIR.

measured or estimated emission factors reported in previous studies.

[65] The completely new emission ratios and emission factors given in this paper for young smoke from savanna fires in southern Africa are for dimethyl sulfide, methyl nitrate, five hydrocarbons (3-methyl-1-butene, *c*-2-pentene, *t*-2-pentene, 2-methyl-1-pentene, and *n*-heptane), and particles with diameters from 0.1 to 3 μm. For all of these

Table 7. Emission Fluxes[a] for Species Whose Emission Factors Have Not Been Reported Previously for African Savanna Fires and Those for Which the Emission Factors Given in This Paper Differ Significantly From Previous Estimates

Species	Savanna in Africa	Savanna Worldwide	All Global Sources
Dimethyl sulfide (C_2H_6S)	2.1 ± 1.8	3.7 ± 3.1	30,000–50,000[b]
Methyl nitrate (CH_3ONO_2)	0.82 ± 0.59	1.44 ± 1.04	
3-methyl-1-butene (C_5H_{10})	8.2 ± 5.4	14.4 ± 9.6	
t-2-pentene (C_5H_{10})	7.2 ± 4.5	12.7 ± 7.9	
c-2-pentene (C_5H_{10})	4.0 ± 2.9	7.1 ± 5.1	
2-methyl-1-pentene (C_6H_{12})	5.6 ± 3.4	9.9 ± 5.9	
n-heptane (C_7H_{16})	11 ± 11	20 ± 20	
Formaldehyde (HCHO)	1,760 ± 610	3,100 ± 1,070	850,000[c]
Ammonia (NH_3)	420 ± 220	730 ± 390	55,000[b]
Hydrogen Cyanide (HCN)	850 ± 240	1,490 ± 420	1,400–2,900[d]
Condensation nuclei (CN)	$(4.8 \pm 2.7) \times 10^{28}$	$(8.5 \pm 4.8) \times 10^{28}$	
Particles 0.1–3.0 μm diameter ($CN_{0.1-3\mu m}$)	$(3.2 \pm 2.4) \times 10^{26}$	$(5.6 \pm 4.2) \times 10^{26}$	

[a]Emission fluxes are measured in Gg yr^{-1}.
[b]*Seinfeld and Pandis* [1998].
[c]From OH oxidation of methane. Industrial combustion emits an unknown quantity [*Hobbs*, 2000].
[d]*Li et al.* [2000].

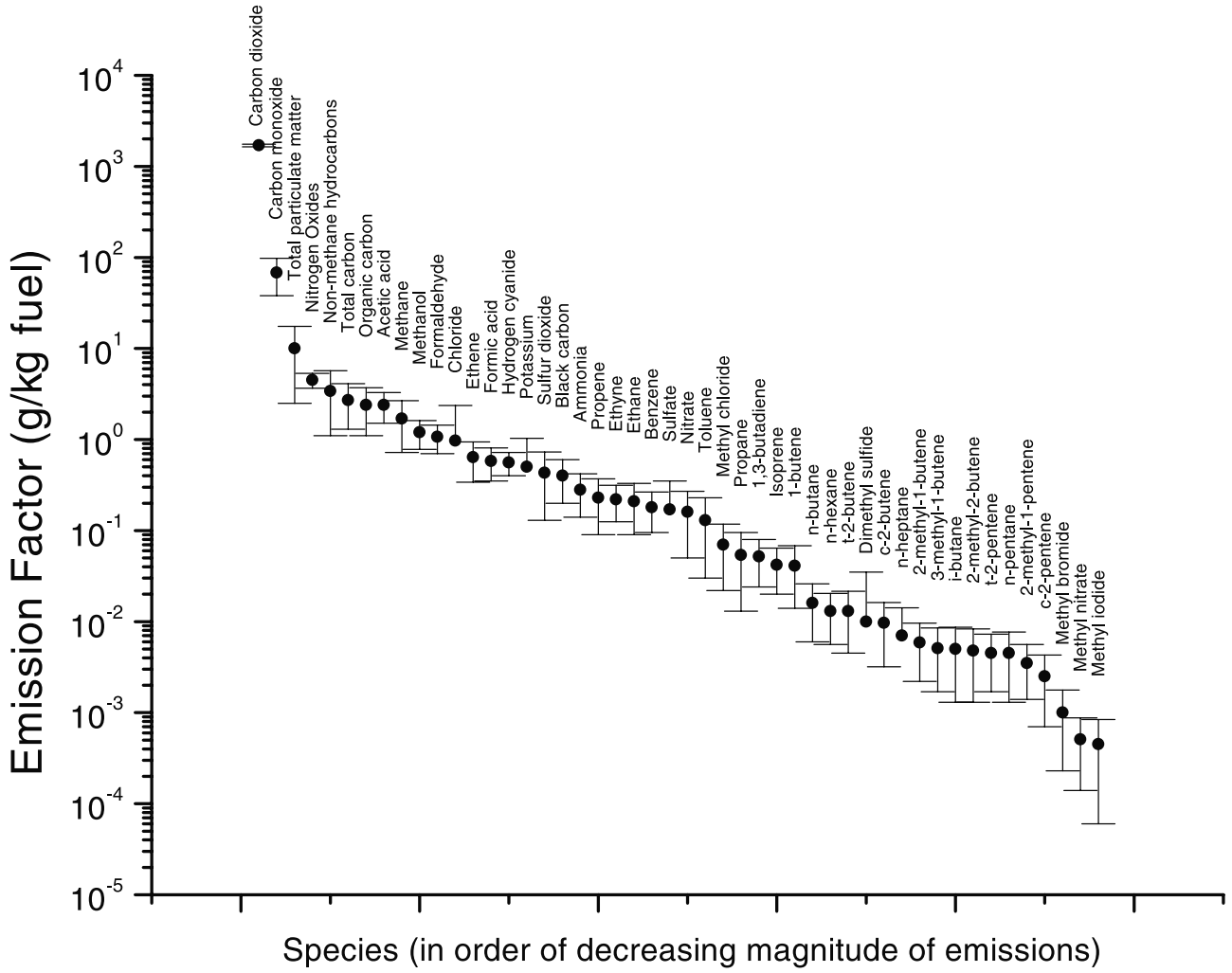

Figure 9. Mean and standard deviations of emission factors for forty-eight gaseous and particulate species based on measurements from 10 savanna fires in southern Africa in this study (see Table 1 for information on the fires). Emission factors for CN and $CN_{0.1-3\ \mu m}$ are not shown.

species the correlation coefficients (r^2) of the excess mixing ratio versus the excess mixing ratio of CO was $\geq$0.5, indicating that they were emitted by the fires. Of particular interest are methyl nitrate, which can redistribute active nitrogen species and lead to ozone formation; the hydrocarbons, which will reduce the concentrations of OH in smoke plumes; and, particles in the accumulation mode, which have long residence times in the atmosphere, can act as cloud condensation nuclei, and promote heterogeneous reactions.

[66] The emission factors reported here that differ significantly from those given for savanna fires by *Andreae and Merlet* [2001] are ammonia, formaldehyde, hydrogen cyanide, and condensation nuclei. Our emission factor for ammonia is about one-fourth that given by Andreae and Merlet, and our emission factors for formaldehyde, hydrogen cyanide, and condensation nuclei are greater by factors of about 3, 20 and 3–15, respectively, than those of Andreae and Merlet. Emissions of formaldehyde, and other oxygenated organic compounds, should increase regional ozone production [*Mason et al.*, 2001]. Abundant hydrogen cyanide emissions support the proposed use of this species, which can be monitored from satellites, for detecting smoke from biomass burning [*Li et al.*, 2000]. Multiplying the average emission factor given here for condensation nuclei, namely, $(3.0 \pm 1.7) \times 10^{16}$ particles per kilogram of fuel burned by the estimate of *Hao and Liu* [1994] of 1600 Tg yr^{-1} for savanna burned in Africa, yields $\sim 2 \times 10^{28}$ to 8×10^{28} particles per year emitted from African savanna fires. This estimate is about a factor of 10 greater than that given by *Le Canut et al.* [1996] for particles emitted worldwide by savanna fires.

[67] The emission factors reported here for total particulate matter, total particulate carbon, organic particulate carbon, and black carbon show large variations from one fire to another. However, our average values for these species do not differ significantly from those given by *Andreae and Merlet* [2001] for savanna fires (see Table 4 and Figure 6).

[68] Emission ratios and emission factors for five species (CO_2, CO, CH_4, C_2H_2, and C_2H_4) were obtained by gas chromatography and Fourier transform infrared spectroscopy. This provided a unique opportunity to compare measurements from two independent techniques under field conditions. Except for C_2H_4, study-average emission ratios

and emission factors obtained by these two methods were not significantly different.

[69] Finally, it should be emphasized that the emission ratios and emission factors given in this paper are for initial smoke, that is, for smoke less than a few minutes old. Many species are transformed as smoke ages. These transformations are discussed in a companion paper [*Hobbs et al.*, 2003].

Appendix A: An Overview of the University of Washington's Airborne Measurements in the SAFARI 2000 Field Study in Southern Africa, by P. V. Hobbs

A1. Introduction

[70] The main goals of the University of Washington (UW) and its guest investigators in the Southern African Regional Science Initiative (SAFARI 2000) were to use its Convair-580 research aircraft facility (Figure A1) to:

1. Measure the physical and chemical properties of aerosols and trace gases in ambient air in the mixed layer and in the free troposphere at various locations in southern Africa.
2. Measure the nature and concentrations of aerosols and trace gases, and their emission factors, in smoke from prescribed and nonprescribed fires of biomass.
3. Obtain measurements on aerosols, trace gases, clouds, and surface properties for comparisons with simultaneous remote sensing measurements from the NASA Terra satellite and ER-2 aircraft, and from SAFARI 2000 ground stations in southern Africa.
4. Measure the spectral albedo and bidirectional reflection distribution function (BRDF) of various surfaces and of clouds in southern Africa.
5. Measure the microstructures of clouds off the South Atlantic Ocean coast of southern Africa.
6. Investigate aerosol-cloud interactions off the South Atlantic Ocean coast of southern Africa.

[71] The field study was carried out from 10 August to 18 September 2000. This is the dry season in southern Africa when biomass burning is widespread. From 10 August to 9 September the Convair-580 was based in Pietersburg, South Africa. During this period twenty-five research flights were carried out over South Africa, Botswana, Zambia and Mozambique. From 10 to 18 September 2000, the Convair-580 was based in Walvis Bay, Namibia, where five flights were made over Namibia and off the west coast of southern Africa.

[72] This appendix provides information on the instrumentation aboard the Convair-580, the aircraft sampling strategies, the flights of the Convair-580 in SAFARI 2000 and their main accomplishments, an overview of some of the ongoing studies of the data collected aboard the Convair-580, and some of the studies of the data yet to be carried out.

A2. Measurements Made Aboard the Convair-580 Aircraft

[73] The instrumentation aboard the UW Convair-580 research aircraft for the SAFARI 2000 field study is listed in Table A1. In addition to the large number of instruments for which the UW was responsible, several instruments were provided by guest investigators (see Table A1).

Figure A1. University of Washington's Convair-580 research aircraft in Pietersburg, South Africa, for SAFARI 2000.

[74] The instrumentation provided measurements of navigational and aircraft flight characteristics; meteorological state parameters (temperature, humidity, winds); comprehensive measurements of aerosol concentrations and size spectra (from 0.01 to 47 μm diameter); light scattering, absorption and extinction; aerosol humidographs; aerosol shape and elemental composition; cloud condensation nuclei (for flights based out of Walvis Bay only); aerosol composition and mass; aerosol optical depths; cloud and precipitation size distributions; cloud liquid water content and cloud droplet effective radius; concentrations of SO_2, O_3, CO_2, CO, NO, NO_x, hydrocarbons, reactive and stable gaseous combustion emissions; column water vapor and ozone; upwelling and downwelling broadband visible, near-infrared, and ultraviolet radiation; solar spectral irradiances and radiances; and, albedos and the bidirectional reflection distribution function (BRDF) of surfaces and clouds.

[75] Some of the instrumentation and techniques used for the aerosol and gas measurements required sampling times longer than it typically took the aircraft to penetrate an individual smoke plume. In this case, a "grab-bag" technique was employed, in which a 2.5 m^3 electrically conducting plastic (Velostat) bag was rapidly filled by ram air. With a 12 s fill time, the bag sampler was able to capture a relatively large volume of smoke over a small distance in the plume. The smoke samples were then drawn through gas and aerosol measuring instruments aboard the aircraft and through filters for subsequent chemical analysis. The grab-bag system had an aerosol 50% cut point diameter of about 4 μm; larger particles were lost in the inlet and on the walls of the grab bag. On many occasions, grab-bag samples were immediately followed by continuous sampling of the ambient air, allowing comparisons between the two.

[76] To avoid possible contamination from the plastic grab-bag material, a different approach was used for obtaining whole air samples of smoke plumes for subsequent analysis of hydrocarbons, halocarbons, dimethyl sulfide, and methyl nitrate. Electropolished stainless steel canisters were filled with air samples from smoke plumes using a stainless steel inlet that passed through the aircraft fuselage.

Table A1. Instrumentation Aboard the University of Washington's Convair-580 Research Aircraft in SAFARI 2000

Parameter	Instrument Type	Manufacturer	Range (and Precision)
	Navigational and Flight Characteristics		
Latitude and longitude	Global Positioning System (GPS)	Trimble TANS/Vector	Global (~2–5 m)
True airspeed	Variable capacitance	Rosemount Model F2VL 781A	0 to 250 m s^{-1} (<0.2%)
True airspeed	Air computer	Shadin	0 to 250 m s^{-1} (<0.2%)
Heading	From TANS/Vector	Trimble TANS/Vector	0 to 360° (±1°)
Pressure	Variable capacitance	Rosemount Model 830 BA	1100 to 150 hPa (<0.2%)
Pressure altitude	Computed from pstat assuming standard atmosphere	–	0–9 km (error depends on atmospheric conditions)
Altitude	Global Positioning System	Trimble TANS/Vector	0–9 km (±15–25 ft)
Altitude above terrain	Radar altimeter	Bendix Model ALA 51A	Up to 0.75 km
Pitch	Differential GPS	Trimble TANS/Vector	0 to 360° (±0.15°)
Roll	Differential GPS	Trimble TANS/Vector	0 to 360° (±0.15°)
	Communications		
Air-to-ground telephone	Via Iridium satellite	Motorola	Worldwide
Air-to-ground e-mail	Via satellite	Magellan	Worldwide
	General Meteorological		
Weather satellite imagery	HF and satellite	ICOM-R8500	Worldwide
Radar reflectivity	3 cm wavelength (pilot's radar)	Bendix/King (now Allied Signal)	250 km
Total air temperature	Platinum wire resistance	Rosemount Model 102CY2CG and 414 L Bridge	−60 to 40°C (<0.1°C)
Total air temperature	Reverse-flow	In-house	−60 to 40°C
Static air temperature	Calculated from Rosemount total temperature	Rosemount Model 102CY2CG and 414 L Bridge	−60 to 40°C
Static air temperature	Reverse-flow thermometer	In-house	−60 to 40°C (<0.5°C)
Dew point temperature	Cooled-mirror dew point	Cambridge System Model TH73-244	−40 to 40°C (<1°C)
Absolute humidity	IR optical hygrometer	Ophir Corp. Model IR-2000	0 to 10 g m^{-3} (~5%)
Wind direction	Calculated from TANS/Vector and Shadin	Trimble	0–360° (0 deg is magnetic north).
Wind speed	Calculated from TANS/Vector and Shadin	Trimble	–
Video image	Forward-looking camera and time code	Ocean Systems Splash Cam	–
	Aerosol		
Number concentration of particles (continuous flow)	Condensation particle counter[a]	TSI Model 3022A	0–107 cm^{-3} (d > 0.003 μm)
Number concentration of particles (continuous flow)	Condensation particle counter	TSI Model 3025A	0–105 cm^{-3} (d > 0.003 μm)
Size spectrum of particles (from grab-bag only)	Differential Mobility Particle Sizing Spectrometer	TSI (modified in-house)	0.01 to 0.6 μm (21 channels)
Size spectrum of particles	35° to 120° light-scattering	Particle Measuring Systems Model PCASP-100X	0.12 to 3.0 μm (15 channels)
Aerodynamic size spectrum of particles and relative light scattering intensity	"Time-of-flight"	TSI Model 3320 APS	0.5–20 μm (52 channels)

Table A1. (continued)

Parameter	Instrument Type	Manufacturer	Range (and Precision)
Light-scattering coefficient ("continuous" measurements on ambient air, but interrupted on occasions for "grab-bag" sampling and humidographs).	Integrating 3-wavelength nephelometer with backscatter shutter	MS Electron 3W-02	1.0×10^{-7} m^{-1} to 1.0×10^{-3} m^{-1} for 550(green) and 700 (red) nm channels. 2.0×10^{-7} m^{-1} to 1.0×10^{-3} m^{-1} for 450 nm channel (blue)
Light-scattering coefficient (grab-bag samples only)	Integrating nephelometer	Radiance Research Model M903	1.0×10^{-6} m^{-1} to 2.0×10^{-4} m^{-1} or 1.0×10^{-6} m^{-1} to 1.0×10^{-3} m^{-1}
Light-scattering coefficient (ambient sampling and extinction cell)	Integrating nephelometer	UW Civil Engineering Dept.	10^{-7} to 10^{-2} m^{-1} at 537 nm
Light absorption and graphitic carbon (continuous measurements on ambient air but interrupted occasionally for grab-bag sampling)	Particle soot absorption photometer	Radiance Research	Absorption coefficient: 10^{-7} to 10^{-2} m^{-1}; Carbon: 0.1–10 mg m^{-3} (±5%)
Humidification factor for aerosol light-scattering (intermittent 5-min scans from either continuous airflow or grab-bag samples)	Scanning humidograph	In-house	b_{sp} (RH) for 30% ≤ RH ≤ 85%
Light-extinction coefficient of smoke (in plumes only)	Optical extinction cell OEC (6 m path length)	In-house	5×10^{-5} to 10^{-2} m^{-1}
Aerosol-shape	Change in light-scattering with applied electric field-Aerosol Asymmetry Analyzer	In-house	Detects 2% deviation from sphericity
Particle size, shape, elemental composition, crystallographic structure, aggregation, etc.	Individual particle analysis using electron-beam techniques (e.g., TEM, EDS, EELS, SAED)[b]	P. R. Buseck (Arizona State Univ.)	Down to a few nanometers
Cloud condensation nucleusspectrum (for Namibia flights only)	Thermal diffusion chamber[b]	Univ. of Wyoming (R. Bruintjes, NCAR)	CCN concentrations at 0.1, 0.3, 0.6 and 1% supersaturation
	Cloud Physics		
Size spectrum cloud particles	Forward light-scattering	Particle Measuring Systems FSSP-100	2 to 47 μm (3 μm)
Liquid water content	Hot wire resistance	Johnson-Williams	0 to 2 or 0 to g m^{-3}
Liquid water content	Hot wire resistance	Droplet Measurement Technologies	0 to 5 g m^{-3}
Size spectrum of particles	Forward light-scattering	Particle Measuring Systems Model FSSP-100	2 to 47 μm (15 channels)
Liquid water content; effective droplet radius; particle surface area	Optical sensor	Gerber Scientific Ins. PVM-100A	LWC = 0.001–10 g m^{-3}
	Chemistry		
SO_2[c]	Pulsed fluorescence	Teco 43S (modified in-house)	1.2 to 200 ppbv (±7%)
O_3[c]	UV absorption	TEI Model 49C	3–1000 ppbv (±1%)
CO_2[c]	Differential IR nondispersive spectrometer	LI-COR Li-6262	2.6 to 1000 ppmv (±15%)
CO[c]	IR gas filter correlation spectrometer	Teco Model 48	62.5–2000 ppbv (±21%)
NO[c]	Chemiluminescence	Modified Monitor Labs. Model 8840	19.3–1000 ppbv (±37%)
NO_x[c]	Chemiluminescence	Modified Monitor Labs. Model 8840	19.3–1000 ppbv (±37%)

Table A1. (continued)

Parameter	Instrument Type	Manufacturer	Range (and Precision)
Total particulate mass and species, $SO_4^=$, NO_3^-, Cl^-, Na, K, Ca, Mg, Fe, carbohydrates, and organic acids	50 Teflon filters, gravimetric analysis, ion chromatography, inductively coupled plasma-atomic emission spectrometry, electrospray ionization source-ion trap mass spectrometer[b]	D. Hegg and S. Gao	Total particulate mass 6–1182 μg m^{-3}
Carbonaceous particles (black and organic carbon)	Quartz filters (Thermal Evolution Techniques)[b]	T. Novakov and T. Kirchstetter (LBNL)	4–160 μg m^{-3} (±1.6 μg m^{-3}) for 1 m^3 sample
CO_2, CO, CH_4, C1–C8 NMHCs, C1–C2 halocarbons, C1–C4 alkyl nitrates, DMS	Collected in stainless steel canisters. Analysis by gas chromatography using flame ionization detector, electron capture detector and mass selective detector.[b]	D. Blake (U.C. Irvine)	Variable
$PM_{2.5}$, $SO_4^=$, NO_3^-, NH_4^+, pH, carbonaceous aerosol	Particle concentrator, organic sampling system (PC-BOSS sampling system)[b]	D. Eatough (Brigham Young University)	–
O_3, CO_2, CO, CH_4, C_2H_4, C_2H_2, CH_3COOH, HCOOH, CH_2O, CH_3OH, HCN, NH_3, NO, NO_2	Fourier transform IR spectrometer (FTIR)[b]	R. Yokelson (U. of Montana)	Single digit ppb to percent
	Radiation		
UV hemispheric radiation, one upward, one downward	Diffuser, filter photo-cell (0.295 to 0.390 μm)	Eppley Lab. Inc. Model TUVR	0 to 70 W m^{-2} (±3 W m^{-2})
VIS-NIR hemispheric radiation (one downward and one upward viewing)	Eppley thermopile (0.3 to 3 μm)	Eppley Lab. Inc. Model PSP	0 to 1400 W m^{-2} (±10 W m^{-2})
Surface radiative temperature	IR radiometer 1.5° FOV (8 to 14 μm)	Omega Engineering OS3701	−50° to 1000°C ±0.8% or reading
Absorption and scattering of solar radiation by clouds and aerosols; reflectivity and BRDF of surfaces	Fourteen wavelength all-directions scanning radiometer	NASA-Goddard/University of Washington (M. King and C. Gatebe, NASA Goddard)	14 discrete wavelengths between 340 and 2300 nm
Solar Spectral irradiance or radiance; Spectral transmission and reflectance	Upward and downward pointed hemispherical signal collectors[b]	NASA Ames Solar Spectral Flux Radiometer (SSFR) (P. Pilewskie, NASA Ames)	300–2500 nm (5–10 nm resolution). FOV 1 mrad. 1 Hz spectral sampling rate.
Aerosol optical depth and water vapor	14-channel Sun-tracking photometer[b]	P. Russell/B. Schmid (NASA Ames)	14 discrete wavelengths, 350–1558 nm

[a]Not connected until UW Flight Number 1823 on August 29, 2000. Connected for flights thereafter.
[b]Guest instrument.
[c]Generally continuous but occasionally interrupted for measurements on grab-bag samples.

Background samples were obtained just upwind of the fires and subtracted from the mixing ratios measured in the smoke samples.

[77] The whole air samples collected in the stainless steel canisters were analyzed by gas chromatography using various techniques (see Table A1). For each sample, mixing ratios of CO_2 (precision of 3%), CO (precision of 10%), CH_4 (precision of 1%), and hydrocarbons with C < 11 (precision of 10%, detection limit of 3 ppt) were measured. The mixing ratios of five halocarbons (CH_3Cl, $CHCl_3$, CH_3I, CH_3Br, and $CHBr_3$) were determined from the canister samples using gas chromatography with an electron capture detector, which were precise to within 10%. Measurements of longer lived halocarbons (CFC, HCFC, and HFC) were accurate to within 2%.

[78] Airborne Fourier transform infrared spectroscopy (AFTIR) was used to measure CO_2, CO, NO_x, CH_4, ethene, acetylene, formaldehyde, acetic acid, formic acid, ammonia, and hydrogen cyanide (HCN) to an accuracy of 1–10%. The AFTIR system design and measurement strategy is described by *Yokelson et al.* [2003].

[79] Particles were collected on quartz and Teflon filters. After gravimetric analysis, the Teflon filters were extracted in deionized water (HPLC grade) and analyzed by a standard ion chromatography system. This analysis yielded mass concentrations of the ions Cl^-, NO_3^-, SO_4^{2-} (precision within 5%) and several organic acid species (precision within 20%) such as oxalate ($C_2O_4^{2-}$). An Inductively Coupled Plasma-Atomic Emission Spectrometer was used to measure the mass concentrations of Na, K, Ca, Mg and Fe (precision of 5%). An electrospray ionization-ion trap mass spectrometer was used to identify and quantify carbohydrate species. Further details on the measurements of water-soluble aerosol components are given by *Gao et al.* [2003].

[80] Aerosol samples collected on the quartz filters were used to determine the concentration of particulate carbon. The quartz filters were baked before use at 800°C for at least 6 h to remove carbonaceous impurities, and then analyzed for total carbon (TC) content using the evolved gas analysis method [*Novakov*, 1981, 1982]. Further details on these procedures are given by *Kirchstetter et al.* [2003].

A3. Airborne Flight Strategies

[81] During the dry season in southern Africa one of the main sources of particles and gases is biomass burning. Therefore, particular attention was paid in SAFARI 2000 to obtaining measurements of the nature and amounts of particles and gases emitted from various types of biomass burning in the region. To this end, we obtained measurements in smoke from 10 fires (six prescribed and four targets of opportunity). In general, the smoke was sampled first close to the fires then at increasing distances downwind. From these measurements, emission factors (i.e., mass of species emitted per unit mass of fuel burned) can be derived using the carbon balance method [*Radke et al.*, 1988], and the transformations of chemical species with smoke age can be determined.

[82] Airborne measurements from the UW Convair-580, obtained simultaneously with a variety of remote sensing measurements from satellites (primarily Terra), from the NASA ER-2 high flying aircraft, and from the ground (at the SAFARI 2000 instrumented sites at Skukusa, South Africa, Inhaca Island, Mozambique, Sua Pan and Maun, Botswana, Mongu, Zambia, and Etosha Pan, Namibia), were an important component of this study. In these cases, continuous measurements of aerosols and a number of gases were obtained, from ~30 m above ground level up to the free troposphere, below and/or above the remote sensing instruments. In addition, during the course of these vertical profiles the aircraft was generally flown back and forth along several horizontal legs ~20–50 km in length at prescribed heights for sufficient periods of time to sample enough air through various filters for subsequent chemical analyses of the aerosols. The measurements obtained in these vertical profiles can be compared with corresponding parameters derived from remote sensing, as well as being used in a variety of column "closure" studies.

[83] Another common flight scenario, generally associated with transiting between sites, were long flights at fairly constant altitudes. Measurements from the continuously recording instruments were made on these flight legs; in addition, filter and canister samples were collected periodically. These data sets provide information on horizontal variabilities in gases, particles and radiation parameters in the mixed layer and free troposphere.

[84] To obtain measurements of BRDF with the NASA-CAR instrument [*King et al.*, 1986; *Gatebe et al.*, 2003], the aircraft was flown in a circle ~2.5 km in diameter at ~650 m above various surfaces and clouds. This provided the complete reflectance pattern of a surface from nadir to horizon and much of the transmittance pattern from zenith to horizon at nine narrow bands in the ultraviolet, visible and infrared.

[85] In flights off the Namibian coast, attention was focused on obtaining in situ measurements of the structures of stratus cloud during overpasses of the NASA ER-2 aircraft and Terra satellite. In these cases, the aircraft flew horizontal legs of ~20 km below cloud base, in cloud, and above cloud top. The leg below cloud base provided measurements of cloud condensation nuclei and aerosols entering the cloud; the in-cloud leg gave measurements of cloud liquid water content and drop size spectra; and the leg above cloud top measurements of the BRDF of the cloud. Also, vertical profiles for physical and chemical measurements were obtained both off the Namibian coast and over Namibia.

A4. Locations of Flights and Overview of Measurements

[86] Figure A2 shows the general locations of the thirty research flights of the Convair-580 in SAFARI 2000. As can be seen, the flights covered a wide area of southern Africa: from Johannesburg, South Africa, in the south to Mongu, Zambia, in the north, and from the Indian Ocean in the east to the South Atlantic Ocean in the west.

[87] Table A2 lists the dates, times, general locations, and the main accomplishments of each of the Convair-580 flights in SAFARI 2000.

A5. Papers in This Special Issue Describing Measurements Obtained Aboard the Convair-580 in SAFARI 2000

[88] This Special Issue of the *Journal of Geophysical Research* contains a number of papers describing measurements obtained aboard the Convair-580 in SAFARI 2000.

Figure A2. Approximate flight tracks (solid lines) of the University of Washington's Convair-580 research aircraft in southern Africa in the SAFARI 2000 field study.

[89] The present paper presents emission ratios and emission factors for a large number of gases and particles emitted by various types of biomass fires in southern Africa. *Yokelson et al.* [2003] used an FTIR aboard the Convair-580 to measure the trace gas composition of nascent, aged, and cloud-processed smoke from savanna fires. The measurements include data on the emissions of oxygenated organic compounds from tropical fires, the formation rate of ozone and acetic acid in tropical biomass-burning plumes, and trace-gas scavenging in cloud-processed smoke. *Gao et al.* [2003] describe the identification and quantification of water-soluble organic compounds and inorganic components in smoke and hazes along with some evolution and distribution patterns. Airborne measurements of carbonaceous particles (black carbon and organic carbon) and semivolatile organic products are described by *Kirchstetter et al.* [2003] and *Eatough et al.* [2003], respectively. The effects of relative humidity on light scattering by particles in ambient air and in the smoke plumes from biomass fires in southern Africa are described by *Magi and Hobbs* [2003]. Detailed information on some of the physical and chemical characteristics of individual particles sampled aboard the Convair-580 in southern Africa are described by *Li et al.* [2003] and *Pósfai et al.* [2003]. *Hobbs et al.* [2003] describe the effects of smoke aging on the trace gases and particles in the plume from a large prescribed biomass fire. *Schmid et al.* [2003] present measurements of column aerosol optical depth (AOD) and water vapor obtained with a multiwavelength Sun photometer aboard the Convair-580. They compare these measurements with ground-based lidar data, with measurements from a downlooking lidar aboard the high-flying NASA ER-2 aircraft, and with satellite retrievals of AOD over land and water. Vertical profiles and aerosol light scattering, light absorption and single-scattering albedo, and comparisons of aerosol optical depths derived from in situ and Sun photometer measurements on the Convair-580, are presented by *Magi and Hobbs* [2003]. Thin, horizontal layers of remarkably clean air, sandwiched between heavily polluted air, were a common feature in southern Africa during SAFARI 2000. *Hobbs* [2003] refers to these layers as ''clean air slots,'' he describes a case study, and offers an explanation for the propensity for clear air slots to occur in

Table A2. Overview of University of Washington's Convair-580 Research Flights In SAFARI 2000

Date, 2000	University of Washington Flight Number	Period of Flight,[a] UTC[b]	General Location	Main Measurements[c]
10 August	1810	1127–1522	About 165 km northwest of Pietersburg, South Africa.	•Physical and chemical measurements above and in boundary layer (23.55°S/28.68°E to 23.09°S/29.28°E).
14 August	1811	1026–1132	Pietersburg to Lanseria, South Africa.	•Measurements en route (23.86°/29.45°E to 25.94°S/27.91°E).
14 August	1812	1216–1505	About 150 km northwest of Johannesburg, South Africa.	•Physical and chemical measurements in boundary layer (24.91°S/27.33°E to 24.84°S/27.49°E). Vertical profile near Lanseria (24.98°S/27.38°E).
14 August	1813	1551–1649	Lanseria to Pietersburg.	•Measurements en route (25.95°S/27.92°E to 23.85°S/29.45°E).
15 August	1814	0655–1115	Pietersburg to Skukusa (in Kruger National Park), South Africa. Then to about 55 km west of Skukusa. Return to Pietersburg.	•Measurements from Pietersburg to Skukusa in free troposphere (at ~2.7 km) en route (23.86°S/29.45°E to 25.01°S/31.56°E). •Runs at an altitude of ~30 m beneath Terra satellite overpass (at 0822 UTC) at Skukusa (24.94°S/31.51°E to 25.00°S/31.31°E). •Physical and chemical measurements at ~910 m just west of Skukusa (25.07°S/31.15°E to 25.02°S/31.12°E). •Measurements of smoke from two grass fires (25.02°S/31.12°E to 24.96°S/31.23°E), and some cumulus sampling, about ~55 km west of Skukusa.
17 August	1815	0701–1213	Pietersburg to south and central Kruger National Park. Return to Pietersburg.	•Measurements en route at ~3 km (24.30°S/30.12°E to 25.09°S/31.30°E). •Vertical profile from ~3 km to ~30 m over Kruger National Park (25.09°S/31.30°E to 25.13°S/31.36°E). •Physical and chemical measurements at ~1.2 km (25.22°S/31.59°E to 25.29°S/31.68°E). •Measurements in two smoke plumes from flaming and smoldering grass fires (25.29°S/31.68°E to 24.44°S/31.70°E). •Measurements on return flight to Pietersburg (24.44°S/31.70°E to 23.87°S/29.44°E).
18 August	1816	0802–1339	Pietersburg to Madikwe Game Reserve (on South Africa/Botswana border) and return.	•Measurements en route (23.86°S/29.45°E to 24.67°S/26.41°E). •Physical and chemical measurements of smoke from prescribed fire in Madikwe Game Reserve (24.67°S/26.41°E to 24.66°S/26.35°E).
20 August	1817	0657–0705	Flight canceled on Pietersburg runway.	N/A
20 August	1818	0713–0819	From Pietersburg west toward South Africa/Botswana border and return.	•Physical and chemical measurements in ambient haze en route (23.86°S/29.45°E to 24.29°S/27.84°E).

Table A2. (continued)

Date, 2000	University of Washington Flight Number	Period of Flight,[a] UTC[b]	General Location	Main Measurements[c]
20 August	1819	1124–1541	Pietersburg to Madikwe Game Reserve and return.	•Physical and chemical measurements in smoke from prescribed fire in Madikwe Game Reserve (24.69°S/26.23°E to 24.29°S/27.76°E). ER-2 passed over fire at 0840 UTC. Terra satellite overpass at 0841 UTC. •Measurements of ambient smoke and haze near Botswana/South Africa border.
22 August	1820	0658–1235	Pietersburg to Skukusa and return to Pietersburg via Phalaborwa, South Africa.	•Vertical profile over Skukusa Airport (24.92°S/31.67°E to 25.04°S/31.57°°E) with ER-2 aircraft and Terra satellite overpasses. •BRDF near Skukusa, South Africa (24.98°S/31.43°E). •BRDF in northern Kruger National Park (24.20°S/31.14°E).
23 August	1821	1138–1448	In vicinity of Pietersburg.	•Intercomparisons of measurements of aerosol and state parameters on Convair-580 with South African Aerocommanders, and with rawinsonde launched from Pietersburg Gateway Airport. •Vertical profile (23.86°S/29.45°E).
24 August	1822	0638–1130	Pietersburg to Inhaca Island, Mozambique.	•Vertical profile over Inhaca Island (25.99°S/32.88°E) with Terra satellite and ER-2 aircraft overpasses.
29 August	1823	0822–1114	From Pietersburg north to South Africa/Zimbabwe border, and return.	•Measurements en route during outbound and return legs (23.75°S/29.36°E to 22.25°S/29.20°E). •Physical and chemical measurements in well mixed boundary layer at ~2.9 km and at ~1.6 km near South Africa/Zimbabwe border (22.81°S/28.86°E to 22.98°S/28.82°E). Terra and TOMS satellite overpasses at 0834 and 0930 UTC, respectively. •BRDF of uniform shrub near El Dorado on South Africa/Zimbabwe border (19.99°S/23.57°E). •Vertical profile near South Africa/Zimbabwe border (22.93°S/28.77°E). •Some cloud penetrations near South Africa/Zimbabwe border (23.45°S/29.09°E to 23.80°S/29.22°E).
29 August	1824	1245–1540	Pietersburg to Skukusa and return.	•BRDF centered on Skukusa tower, Kruger National Park (25.03°S/31.51°E). •Measurements of smoke from small smoldering fire in Kruger National Park (25.17°S/31.40°E). (Also sampled older smoke on flight back to Pietersburg.) •~60 m run over plantations on high veldt (24.84°S/30.88°E).

Table A2. (continued)

Date, 2000	University of Washington Flight Number	Period of Flight,[a] UTC[b]	General Location	Main Measurements[c]
31 August	1825	0842–1421	Pietersburg to central Mozambique coast. North along Mozambique coastline to west of Beira. Return to Pietersburg.	•Measurements at several levels on transit legs (23.88°S/29.34°E to 21.90°S/35.33°E). •Run at ~30 m along Mozambique coastline (21.90°S/35.33°E to 21.47°S/35.17°E). •Measurements of smoke at several distances downwind from smoldering fire west of Beira, Mozambique (20.97°S/34.65°E to 21.23°S/34.67°E). •Good measurements in haze and smoke on return flight (21.23°S/34.67°E to 23.72°S/30.71°E). •Vertical profile on return flight to Pietersburg (23.72°S/30.71°E to 23.89°S/29.46°E).
1 September	1826	0532–1108	Pietersburg to Kaoma, Zambia, to Kasane, Botswana.	•Measurements en route to Kaoma (23.42°S/29.26°E to 14.81°S/24.47°E).at 0902 UTC. •Detailed measurements on prescribed Miombo burn near Kaoma, Zambia (14.82°S/24.46°E to 14.80°S/24.44°E). Terra satellite overpass at 0902 UTC •Vertical profile out of Kaoma (14.80°S/24.44°E to 15.55°S/24.66°E). •Measurements en route from Kaoma to Kasane (15.55°S/24.66°E to 17.25°S/25.04°E). •Vertical profile on descent to Kasane (17.25°S/25.04°E to 17.69°S/25.12°E).
1 September	1827	1229–1241	Did not take off from Kasane, Botswana.	–
1 September	1828	1329–1551	Kasane to Pietersburg.	•Measurements en route from Kasane to Pietersburg (18.06°S/25.19°E to 23.78°S/29.40°E).
2 September	1829	0736–1334	Pietersburg to Maun, Botswana, and return to Pietersburg.	•BRDF centered on Maun tower (20.00°S/23.53°E). •Vertical profile under TOMS satellite at Maun tower (20.01°S/23.57°E to 20.45°S/24.41°E).
3 September	1830	0702–1238	Pietersburg to Sua Pan, Botswana, and return.	•BRDF over Sua Pan and grass (20.65°S/25.89°E to 20.65°S/26.19°E). •Vertical profile over Sua Pan parabola site (20.72°S/25.80°E to 20.54°S/26.46°E) with Terra satellite overpass at 0852 UTC. •Measurements at several altitudes on transit legs (20.54°S/26.46°E to 23.87°S/29.46°E).
5 September	1831	0838–1413	Pietersburg to Kaoma to Kasane via Senanga, Zambia.	•Measurements from Pietersburg to Kaoma (23.79°S/29.46°E to 14.96°S/24.48°E). •Measurements on smoke from prescribed burn of Dambo near Kaoma (14.78°S/24.47°E to 14.68°S/24.56°E). •Measurements en route to Kasane with low-level pass over Senanga, Zambia (19.68°S/24.56°E to 17.83°S/25.17°E).

Table A2. (continued)

Date, 2000	University of Washington Flight Number	Period of Flight,[a] UTC[b]	General Location	Main Measurements[c]
6 September	1832	0700–1058	Kasane to ~20 miles north of Mongu, Zambia. Return to Kasane.	•Low-level run from Senanga, Zambia, to Mongu to about ~37 km north of Mongu (16.01°S/23.26°E to 14.86°S/23.08°E). •BRDF over Mongu tower (15.44°S/23.26°E). •Vertical profile over Mongu (15.32°S/23.18°E to 15.17°S/23.18°E) airport. ER-2 overflight at 0900 UTC. •Measurements en route back to Kasane (15.17°S/23.18°E to 17.84°S/25.15°E).
6 September	1833	1133–1354	Kasane to Pietersburg.	•Measurements in boundary layer from Kasane to Pietersburg (17.90°S/25.21° to 23.84°S/29.46°).
7 September	1834	0755–1220	Pietersburg to Timbavati Game Reserve (near Kruger National Park, South Africa) to Phalaborwa, South Africa, and return to Pietersburg.	•Extensive measurements on large prescribed fire in Timbavati Game Reserve (24.05°S/30.24°E to 23.74°S/31.61°E) with Terra satellite overpass at 0828 UTC and ER-2 aircraft overflights at 0828, 1145 and 1205 UTC. •Two intercepts of plume from Phalaborwa copper mine (23.96°S/31.18°E to 23.96°S/31.15°E). •Two sets of BRDF on Mopane trees (23.73°S/31.62°E to 23.58°S/31.49°E).
10 September	1835	0558–1025	Pietersburg to Walvis Bay, Namibia.	•Measurements en route (23.86°S/29.45°E to 22.98°S/14.66°E).
11 September	1836	0835–1222	Walvis Bay to off central Namibian coast; then to Kuiseb Desert, Namibia. Return to Walvis Bay.	•Underflew Terra satellite overpass (at 0942 UTC) and ER-2 aircraft overpass (at 0942 UTC) in thin, scattered stratus cloud off central Namibia coast (23.03°S/14.44°E to 22.67°S/12.11°E). •Vertical profile to ~3.7 km off central Namibia coast (22.67°S/12.11°E to 23.55°S/12.71°E) for Sun photometer and in situ comparisons. •Two sets of five CAR turns for BRDF measurements of sky and "red" sand in Kuiseb Desert, south of Walvis Bay (23.37°S/14.59°E to 23.38°S/14.65°E).
13 September	1837	0826–1416	Walvis Bay to off Namibian coast. Return to Walvis Bay.	•Measurements below, above and in stratus off Namibian coast (22.89°S/14.66°E to 20.30°S/13.16°E) under Terra satellite overpass (at 0930 UTC) and ER-2 aircraft overpass (at 0930 UTC). •Vertical profile, with physical and chemical measurements, from cloud top to ~5.1 km (20.30°S/13.16°E to 20.11°S/13.26°E). •Two sets of BRDF measurements on stratus clouds (20.64°S/13.13°E to 20.49°S/13.12°E).

Table A2. (continued)

Date, 2000	University of Washington Flight Number	Period of Flight,[a] UTC[b]	General Location	Main Measurements[c]
14 September	1838	0800–1232	Walvis Bay to off west coast of South Africa. Return to Walvis Bay.	•Measurements on post-frontal cumulus congestus, including inflow, outflow, and below cloud base measurements (26.62°S/14.12°E to 26.36°S/13.90°E). •Measurements of effluents from two freighter ships (26.27°S/13.47°E to 25.88°S/13.87°E). •Vertical profile to ~3.7 km for Sun photometer and in situ measurements (25.36°S/13.92°E to 25.36°S/13.95°E). •Measurements through dust storm on descent into Walvis Bay (23.16°S/14.61°E to 22.98°S/14.65°E).
16 September	1839	0709–1245	Walvis Bay to Etosha National Park, Namibia. Return to Walvis Bay.	•BRDF of white Etosha pan (at 19.05°/15.96°) and of Mopane trees (at 19.18° south/15.66° east) in Etosha National Park (18.98°S/15.99°E to 18.99°S/16.04°E). •Vertical profile from ~60 m to 4.8 km (19.18°S/15.86°E to 19.22°S/15.92°E) over ground-based Sun photometer site in Etosha (at 19°11′ south/15°55′ east). •Measurements in and below small cumulus clouds near Walvis Bay (22.55°S/14.84°E to 22.98°S/14.65°E).

[a]Engines on to engines off.
[b]Local time = UTC + 2 hours.
[c]All heights are above mean sea level.

southern Africa during the dry season. *Pilewskie et al.* [2003] utilize the spectral radiometer measurements from the SSFR (see Table A1) to derive the effects on radiative forcing of aerosols in southern Africa during SAFARI 2000. Measurements of the BRDF and hemispherical albedo of various surfaces in southern Africa, obtained aboard the UW Convair-580, are described by *Gatebe et al.* [2003]. Some comparisons between in situ measurements of CO aboard the Convair-580 and scanning high-resolution interferometer sounder (SHIS) aboard the ER-2 aircraft are discussed by *McMillan et al.* [2003].

A6. Future Studies

[90] Many studies remain to be carried out utilizing data collected aboard the Convair-580 in SAFARI 2000. These studies include:

1. In situ and remote sensing measurements of vertical profiles of light scattering, light absorption and light extinction were obtained aboard the Convair-580. These measurements need to be documented and compared with each other, and with remote sensing measurements from the ground, from satellites, and from the overflying NASA ER-2 aircraft.

2. Transformations of chemicals in southern Africa over both short (hours) and long (days) time periods, and in cloud-free and cloudy situations, can be explored with the data obtained on the Convair-580.

3. Measurements of the smoke from several prescribed and nonprescribed biomass fires in South Africa, Mozambique, Botswana and Zambia have yet to be studied in detail.

4. Modeling of emissions from biomass fires and their transformations and comparisons with measurements obtained aboard the Convair-580 in SAFARI 2000.

5. The spectral and broadband albedo (and BRDF) of various surfaces and clouds in southern Africa.

6. Transformations of pollutants from the interior of southern Africa to the South Atlantic Ocean.

7. The microstructures of stratus and cumulus clouds off the Namibian coast, and comparisons of the in situ airborne measurements with simultaneous remote sensing measurements from the NASA ER-2 aircraft and the Terra satellite.

8. Vertical profiles of particles and gases through a number of clean air slots should be studied in an effort to determine the mechanisms by which such slots are maintained over long time periods and over large areas.

9. Analyses of the emissions from two tanker ships, which were measured off the Namibian coast.

[91] **Acknowledgments.** We thank all members of the UW-CARG for help in obtaining measurements, and Dan Jaffe for help in calibrating the gas instruments. Thanks are also due to the organizers of the SAFARI 2000 Southern African Regional Science Initiative, and all those on the ground and in the field, who contributed to this study. This research was supported by grants NAG5-9022 and NAG5-7675 from NASA's Radiation Science Program, grants NCC5-550 and NASI-18940 from the NASA EOS Program, and grants ATM-9901624 and ATM-9900494 from NSF's Division of Atmospheric Sciences.

References

Andreae, M. O., and P. Merlet, Emission of trace gases and aerosols from biomass burning, *Global Biogeochem. Cycles*, *15*, 955–966, 2001.

Andreae, M. O., E. Atlas, H. Cachier, W. R. Cofer III, G. W. Harris, G. Helas, R. Koppmann, J. Lacaux, and D. Ward, Trace gas and aerosol emissions from savanna fires, in *Biomass Burning and Global Change*, vol. 1, edited by J. S. Levine, pp. 278–295, MIT Press, Cambridge, Mass., 1996.

Andreae, M. O., et al., Airborne studies of aerosol emissions from savanna fires in southern Africa: Aerosol chemical composition, *J. Geophys. Res.*, *103*, 32,114–32,128, 1998.

Bertschi, I., R. J. Yokelson, D. E. Ward, J. G. Goode, R. Babbitt, R. A. Susott, and W. M. Hao, Trace gas and particle emissions from fires in large diameter and belowground biomass fuels, *J. Geophys. Res.*, *108*(D13), 8472, doi:10.1029/2002JD002100, 2003.

Blake, N. J., D. R. Blake, B. C. Sieve, T.-Y. Chen, F. S. Rowland, J. E. Collins Jr., G. W. Sachse, and B. E. Anderson, Biomass burning emissions and vertical distribution of atmospheric methyl halides and other reduced carbon gases in the South Atlantic region, *J. Geophys. Res.*, *101*, 24,151–24,164, 1996.

Cachier, H., C. Liousse, M. Pertuisot, A. Gaudichet, F. Echalar, and J. Lacaux, African fire particulate emissions and atmospheric influence, in *Biomass Burning and Global Change*, vol. 1, edited by J. S. Levine, pp. 428–440, MIT Press, Cambridge, Mass., 1996.

Cofer, W. R., III, J. S. Levine, E. L. Winstead, D. R. Cahoon, D. I. Sebacher, J. P. Pinto, and B. J. Stocks, Source composition of trace gases released during African savanna fires, *J. Geophys. Res.*, *101*, 23,597–23,602, 1996.

Colman, J. J., A. L. Swanson, S. Meinardi, B. C. Sive, D. R. Blake, and F. S. Rowland, Description of the analysis of a wide range of volatile organic compounds in whole air samples collected during PEM-Tropics A and B, *Anal. Chem.*, *73*, 3723–3731, 2001.

Crutzen, P. J., and M. O. Andreae, Biomass burning in the tropics: Impact on atmospheric chemistry and biogeochemical cycles, *Science*, *250*, 1669–1678, 1990.

Delmas, R., On the emission of carbon, nitrogen and sulfur in the atmosphere during bushfires in intertropical savannah zones, *Geophys. Res. Lett.*, *9*, 761–764, 1982.

Eatough, D. J., N. L. Eatough, Y. Pang, S. Sizemore, T. W. Kirchstetter, T. Novakov, and P. V. Hobbs, Semivolatile particulate organic material in southern Africa during SAFARI 2000, *J. Geophys. Res.*, *108*(D13), 8479, doi:10.1029/2002JD002296, 2003.

Ferek, R. J., J. S. Reid, P. V. Hobbs, D. R. Blake, and C. Liousse, Emission factors of hydrocarbons, halocarbons, trace gases and particles from biomass burning in Brazil, *J. Geophys. Res.*, *103*, 32,107–32,118, 1998.

Fishman, J., K. Fakhruzzaman, B. Cros, and D. Nganga, Identification of widespread pollution in the southern hemisphere deduced from satellite analyses, *Science*, *252*, 1693–1696, 1991.

Fishman, J., J. M. Hoell, R. D. Bendura, R. J. McNeil, and V. W. J. H. Kirchhoff, NASA GTE TRACE A experiment (Sept.–Oct. 1992): Overview, *J. Geophys. Res.*, *101*, 23,869–23,879, 1996.

Gao, S., D. A. Hegg, P. V. Hobbs, T. W. Kirchstetter, B. I. Magi, and M. Sadilek, Water-soluble organic components in aerosols associated with savanna fires in southern Africa: Identification, evolution and distribution, *J. Geophys. Res.*, *108*, doi:10.1029/2002JD002324, in press, 2003.

Gatebe, C. K., M. D. King, S. Platnick, G. T. Arnold, E. F. Vermote, and B. Schmid, Airborne spectral measurements of surface-atmosphere anisotropy for several surfaces and ecosystems over southern Africa, *J. Geophys. Res.*, *108*, doi:10.1029/2002JD002397, in press, 2003.

Goode, J. G., R. J. Yokelson, R. A. Susott, and D. E. Ward, Trace gas emissions from laboratory biomass fires measured by open-path Fourier transform infrared spectroscopy: Fires in grass and surface fuels, *J. Geophys. Res.*, *104*, 21,237–21,245, 1999.

Goode, J. G., R. J. Yokelson, D. E. Ward, R. A. Susott, R. E. Babbitt, M. A. Davis, and W. M. Hao, Measurements of excess O_3, CO_2, CO, CH_4, C_2H_4, C_2H_2, HCN, NO, NH_3, HCOOH, CH_3COOH, HCHO and CH_3OH in 1997 Alaskan biomass burning plumes by airborne Fourier transform infrared spectroscopy (AFTIR), *J. Geophys. Res.*, *105*, 22,147–22,166, 2000.

Gundel, L. A., R. L. Dod, H. Rosen, and T. Novakov, The relationship between optical attenuation and black carbon concentrations for ambient and source particles, *Sci. Total Environ.*, *36*, 197–202, 1984.

Hao, W. M., and M. H. Liu, Spatial and temporal distribution of tropical biomass burning, *Global Biogeochem. Cycles*, *8*, 495–503, 1994.

Herring, J. A., Radiative properties, dynamics and chemical evolution of the smoke from the 1991 Kuwait oil fires, Ph.D. dissertation, 301 pp., Univ. of Wash., Seattle, 1994.

Hobbs, P. V., *Introduction to Atmospheric Chemistry*, Cambridge Univ. Press, New York, 2000.

Hobbs, P. V., Clean air slots amid dense atmospheric pollution in southern Africa, *J. Geophys. Res.*, *108*, doi:10.1029/2002JD002156, in press, 2003.

Hobbs, P. V., P. Sinha, R. J. Yokelson, T. J. Christian, D. R. Blake, S. Gao, T. W. Kirchstetter, T. Novakov, and P. Pilewskie, Evolution of gases and particles from a savanna fire in South Africa, *J. Geophys. Res.*, *108*, doi:10.1029/2002JD002352, in press, 2003.

Hurst, D. F., D. W. T. Griffith, J. N. Carras, D. J. Williams, and P. J. Fraser, Measurements of trace gases emitted by Australian savanna fires during the 1990 dry season, *J. Atmos. Chem.*, *18*, 33–56, 1994.

King, M. D., M. G. Strange, P. Leone, and L. R. Blaine, Multiwavelength scanning radiometer for airborne measurements of scattered radiation in clouds, *J. Atmos. Oceanic Technol.*, *3*, 513–522, 1986.

Kirchstetter, T. W., C. E. Corrigan, and T. Novakov, Laboratory and field investigation of the adsorption of gaseous organic compounds onto quartz filters, *Atmos. Environ.*, *35*, 1663–1671, 2001.

Kirchstetter, T. W., T. Novakov, P. V. Hobbs, and B. Magi, Airborne measurements of carbonaceous aerosols in southern Africa during the dry biomass burning season, *J. Geophys. Res.*, *108*(D13), 8476, doi:10.1029/2002JD002171, 2003.

Kliner, D. A. V., B. C. Daube, J. D. Burley, and S. C. Wofsy, Laboratory investigation of the catalytic reduction NO_y, *J. Geophys. Res.*, *102*, 10,759–10,776, 1997.

Lacaux, J., R. A. Delmas, B. Cros, B. Lefeivre, and M. O. Andreae, Influence of biomass burning on precipitation chemistry in the equatorial forests of Africa, in *Global Biomass Burning*, edited by J. S. Levine, pp. 167–173, MIT Press, Cambridge, Mass., 1991.

Le Canut, P., M. O. Andreae, G. W. Harris, F. G. Wienhold, and T. Zenker, Airborne studies of emissions from savanna fires in southern Africa, 1, Aerosol emissions measured with a laser optical particle counter, *J. Geophys. Res.*, *101*, 23,615–23,630, 1996.

Li, B. Q., D. J. Jacob, I. Bey, R. M. Yantosca, Y. J. Zhao, Y. Kondo, and J. Notholt, Atmospheric hydrogen cyanide (HCN): Biomass burning source, ocean sink?, *Geophys. Res. Lett.*, *27*, 357–360, 2000.

Li, J., M. Pósfai, P. V. Hobbs, and P. R. Buseck, Individual aerosol particles from biomass burning in southern Africa: 2. Compositions and aging of inorganic particles, *J. Geophys. Res.*, *108*, doi:10.1029/2002JD002310, in press, 2003.

Lobert, J. M., W. C. Keene, J. A. Logan, and R. Yevich, Global chlorine emissions from biomass burning: Reactive chlorine emissions inventory, *J. Geophys. Res.*, *104*, 8373–8389, 1999.

Logan, J. A., M. J. Prather, S. C. Wofsy, and M. B. McElroy, Tropospheric chemistry: A global perspective, *J. Geophys. Res.*, *86*, 7210–7254, 1981.

Magi, B. I., and P. V. Hobbs, The effects of humidity on aerosols in southern Africa during the biomass burning season, *J. Geophys. Res.*, *108*, doi:10.1029/2002JD002144, in press, 2003.

Magi, B., P. V. Hobbs, B. Schmid, and J. Redemann, Vertical profiles of light scattering, light absorption, and single-scattering albedo during the dry, biomass burning season in southern Africa and comparisons of in situ and remote sensing measurements of aerosol optical depths, *J. Geophys. Res.*, *108*, doi:10.1029/2002JD002361, in press, 2003.

Mano, S., and M. O. Andreae, Methyl bromide from biomass burning, *Science*, *263*, 1255–1256, 1994.

Mason, S. A., R. J. Field, R. J. Yokelson, M. A. Kochivar, M. R. Tinsley, D. E. Ward, and W. M. Hao, Complex effects arising in smoke plume simulations due to inclusion of direct emissions of oxygenated organic species from biomass combustion, *J. Geophys. Res.*, *106*, 12,527–12,539, 2001.

Mazurek, M. A., W. R. Cofer III, and J. S. Levine, Carbonaceous aerosols from prescribed burning of a boreal forest ecosystem, in *Global Biomass Burning: Atmospheric, Climatic and Biospheric Implications*, edited by J. S. Levine, pp. 258–263, MIT Press, Cambridge, Mass., 1991.

McKenzie, L. M., D. E. Ward, and W. M. Hao, Chlorine and bromine in the biomass of tropical and temperate ecosystems, in *Biomass Burning and Global Change*, vol. 1, edited by J. S. Levine, pp. 240–248, MIT Press, Cambridge, Mass., 1996.

McMillan, W. W., et al., Tropospheric carbon monoxide measurements from the Scanning High-Resolution Interferometer Sounder on 7 September 2000, in southern Africa during SAFARI 2000, *J. Geophys. Res.*, *108*, doi:10.1029/2002JD002335, 2003.

Novakov, T., Microchemical characterization of aerosols, in *Nature, Aim and Methods of Microchemistry*, edited by H. Malissa, M. Grasserbaure, and R. Belcher, pp. 141–165, Springer-Verlag, New York, 1981.

Novakov, T., Soot in the atmosphere, in *Particulate Carbon: Atmospheric Life Cycle*, edited by G. T. Wolff and R. L. Klimish pp. 19–41, Plenum, New York, 1982.

Pilewskie, P., J. Pommier, R. Bergstrom, W. Gore, S. Howard, M. Robbette, B. Schmid, P. V. Hobbs, and S.-C. Tsay, Solar spectral radiative forcing during the Southern African Regional Science Initiative, *J. Geophys. Res.*, *108*, doi:10.1029/2002JD002411, in press, 2003.

Pósfai, M., R. Simonics, J. Li, P. V. Hobbs, and P. B. Buseck, Individual aerosol particles from biomass burning in southern Africa: 1. Compositions and size distributions of carbonaceous particles, *J. Geophys. Res.*, *108*, doi:10.1029/2002JD002291, in press, 2003.

Quay, P. D., et al., Carbon isotopic composition of atmospheric methane: Fossil and biomass burning strengths, *Global Biogeochem. Cycles*, *5*, 25–47, 1991.

Radke, L. F., D. A. Hegg, J. H. Lyons, C. A. Brock, and P. V. Hobbs, Airborne measurements on smokes from biomass burning, in *Aerosols and Climate*, edited by P. V. Hobbs and M. P. McCormick, pp. 411–422, A. Deepak, Hampton, Va., 1988.

Reid, J. S., P. V. Hobbs, R. J. Ferek, D. R. Blake, J. V. Martins, M. R. Dunlap, and C. Liousse, Physical, chemical, and optical properties of regional hazes dominated by smoke in Brazil, *J. Geophys. Res.*, *103*, 32,059–32,080, 1998.

Rodgers, C. F., J. G. Hudson, B. Zielinska, R. L. Tanner, J. Hallett, and J. G. Watson, Cloud condensation nuclei from biomass burning, in *Global Biomass Burning*, edited by J. S. Levine, pp. 431–438, MIT Press, Cambridge, Mass., 1991.

Rosen, H., and T. Novakov, Optical-transmission through aerosol deposits on diffusely reflective filters—A method for measuring the absorbing component of aerosol-particles, *Appl. Opt.*, *22*, 1265–1267, 1983.

Schmid, B., et al., Coordinated airborne, spaceborne, and ground-based measurements of massive, thick aerosol layers during the dry season in southern Africa, *J. Geophys. Res.*, *108*, doi:10.1029/2002JD002297, in press, 2003.

Seinfeld, J. H., and S. N. Pandis, *Atmospheric Chemistry and Physics*, John Wiley, New York, 1998.

Susott, R. A., G. J. Olbu, S. P. Baker, D. E. Ward, J. B. Kauffmann, and R. W. Shea, Carbon, hydrogen, nitrogen, and thermogravimetric analysis of tropical ecosystem biomass, in *Biomass Burning and Global Change*, vol. 1, edited by J. S. Levine, pp. 249–259, MIT Press, Cambridge, Mass., 1996.

Thompson, A. M., K. E. Pickering, D. P. McNamara, M. R. Schoeberl, R. D. Hudson, J. H. Kim, E. V. Browell, V. W. J. H. Kirchhoff, and D. Nganga, Where did tropospheric ozone over southern Africa and the tropical Atlantic come from in October 1992? Insights from TOMS, GTE TRACE A, and SAFARI 1992, *J. Geophys. Res.*, *101*, 24,251–24,278, 1996.

Turpin, B. J., J. J. Huntzicker, and S. V. Hering, Investigation of the organic aerosol sampling artifacts in the Los Angeles basin, *Atmos. Environ.*, *28*, 3061–3071, 1994.

Ward, D. E., and W. M. Hao, Air toxic emissions from burning of biomass globally—Preliminary estimates, paper presented at Annual Meeting and Exhibition, Air and Waste Management Association, Vancouver, British Columbia, 1992.

Ward, D. E., and C. C. Hardy, Smoke emissions from wildland fires, *Environ. Int.*, *17*, 117–134, 1991.

Ward, D. E., and L. F. Radke, Emissions measurements from vegetation fires: A comparative evaluation of methods and results, in *Fire in the Environment: The Ecological, Atmospheric, and Climatic Importance of Vegetation Fires*, edited by P. J. Crutzen and J. G. Goldammer, pp. 53–76, John Wiley, New York, 1993.

Warneck, P., *Chemistry of the Natural Atmosphere*, Academic, San Diego, Calif., 2000.

White, F., *UNESCO/AETFAT/UNSO Vegetation Map of Africa*, UNESCO, Paris, 1981.

White, F., *Vegetation of Africa*, UNESCO, Paris, 1983.

Winklmayer, W., G. P. Reischl, A. O. Lindner, and A. Berner, A new electromobility spectrometer for the measurement of the aerosol size distributions in the size ranges of 1 to 1,000 nm, *J. Geophys. Res.*, *22*, 289–296, 1991.

Yokelson, R. J., D. W. T. Griffith, and D. W. Ward, Open-path Fourier transform infrared studies of large-scale laboratory biomass fires, *J. Geophys. Res.*, *101*, 21,067–21,080, 1996.

Yokelson, R. J., J. G. Goode, D. E. Ward, R. A. Susott, R. E. Babbitt, D. D. Wade, I. Bertschi, W. W. T. Griffith, and W. M. Hao, Emissions of formaldehyde, acetic acid, methanol, and other trace gases from biomass fires in North Carolina measured by airborne Fourier transform infrared spectroscopy, *J. Geophys. Res.*, *104*, 30,109–32,125, 1999.

Yokelson, R. J., I. T. Bertschi, T. J. Christian, P. V. Hobbs, D. E. Ward, and W. M. Hao, Trace gas measurements in nascent, aged, and cloud-processed smoke from African savanna fires by airborne Fourier transform infrared spectroscopy (AFTIR), *J. Geophys. Res.*, *108*(D13), 8478, doi:10.1029/2002JD002322, 2003.

I. T. Bertschi, Interdisciplinary Arts and Sciences, University of Washington, 18115 Campus Way NE, Bothell, WA 98011, USA. (isaacpb@u.washington.edu)

D. R. Blake and I. J. Simpson, Department of Chemistry, University of California, Irvine, CA 92697, USA. (dblake@orion.oac.uci.edu; isimpson@uci.edu)

S. Gao, Department of Chemistry, University of Washington, Box 351700, Seattle, WA 98195-1700, USA. (sgao@u.washington.edu)

P. V. Hobbs (corresponding author) and P. Sinha, Department of Atmospheric Sciences, University of Washington, Box 351640, Seattle, WA 98195-1640, USA. (phobbs@atmos.washington.edu; psinha@atmos.washington.edu)

T. W. Kirchstetter and T. Novakov, Lawrence Berkeley National Laboratory, 1 Cyclotron Road, Berkeley, CA 94720, USA. (twkirchstetter@lbl.gov; tnovakov@lbl.gov)

R. J. Yokelson, Department of Chemistry, University of Montana, Missoula, MT 59812, USA. (byok@selway.umt.edu)